# PHYLOGENY OF *CHILICOLA (HYLAEOSOMA)* (HYMENOPTERA: COLLETIDAE) BASED ON MORPHOLOGICAL AND MORPHOMETRIC DATA OF EXTANT AND FOSSIL SPECIES, WITH DESCRIPTION OF SEVEN NEW SPECIES

**MARGARITA MIKLASEVSKAJA**

**A thesis submitted to**
**the Faculty of Graduate Studies**
**in partial fulfillment of the requirements**
**for the degree of**

**Master of Science**

**Graduate Program in Biology**
**York University**
**Toronto, Ontario, Canada**

**Oct 2017**

## ABSTRACT

Combined data approach is used to establish a phylogeny of the bee subgenus *Chilicola (Hylaeosoma)* Ashmead 1898 (Colletidae: Xeromelissinae). Results of phylogenetic analyses are presented, based upon 92 morphological characters and 3 wing landmark shape configurations. Monophyly of the subgenus is supported. *Chilicola longiceps* Ashmead 1898 is grouped with *megalostigma* morphogroup and renders *longiceps* morphogroup paraphyletic. Two *C. (Hylaeosoma)* fossils are nested within the tree with *C. electrodominica* Engel 1999 occupying a more derived position than *C. gracilis* Michener and Poinar 1995. Effectiveness and reliability of continuous characters is discussed and compared to other methods. Seven new species are described: *Chilicola (Hylaeosoma) herberti* Miklasevskaja **sp. nov.**, *Chilicola (Hylaeosoma) rufotergata* Miklasevskaja **sp. nov.**, *Chilicola (Hylaeosoma) paveli* Miklasevskaja **sp. nov.**, *Chilicola (Hylaeosoma) liudmilae* Miklasevskaja **sp. nov.**, *Chilicola (Hylaeosoma) boyacense* Miklasevskaja **sp. nov.**, *Chilicola (Hylaeosoma) boliviana* Miklasevskaja **sp. nov.**, *Chilicola (Hylaeosoma) lambayequense* Miklasevskaja **sp. nov.**.

## ACKNOWLEDGEMENTS

First and foremost, I would like to express my sincere gratitude to Dr. Laurence Packer for his motivation, mentorship, and support. His guidance and immense knowledge helped me tremendously throughout research and writing of this thesis. His patience and understanding are remarkable and had helped make this experience stress-free and enjoyable.

This work could not have been done without specimens from the American Museum of Natural History (AMNH), Kansas University Biodiversity Institute and the Bee Biology and Systematics Laboratory (BBSL).

I thank my fellow lab mates, Rafael Ferrari and Tom Onuferko for their invaluable input and stimulating discussions. Last but not the least, I would like to thank my family and friends for supporting me throughout this thesis.

## DISCLAIMER

All names and nomenclatural acts in this document are disclaimed for nomenclatural purposes, and shall not be considered available upon dissemination of this thesis. This disclaimer is included in accordance with Article 8.3 of the International Code of Zoological Nomenclature, and is pursuant to the author's intent to publish these names and nomeclatural acts in a widely distributed and peer-reviewed scientific journal.

## TABLE OF CONTENTS

## LIST OF TABLES

## LIST OF FIGURES

## INTRODUCTION

Bees (Apoidea) constitute a monophyletic group that arose from apoid wasps (Michener 1979, Melo 1999, Engel 2001, Ohl and Bleidorn 2006, Danforth and Poinar 2011, Branstetter et al. 2016). This transition was at large promoted by a shift in feeding habits from animal food sources to pollen as a main source of protein (Michener 1979, Engel 2001). While monophyly of Apoidea has been long agreed on (Brothers 1999, Branstetter et al. 2016), the phylogeny within the bee lineage itself has been rather controversial (Roig-Alsina and Michener, 1993, Alexander and Michener 1995, Danforth et al. 2006, Brady et al. 2011, Debevec et al. 2012, Hedtke 2013, Branstetter et al. 2016).

Traditionally, bees are separated into long-tongued and short-tongued families (Michener 1979). Short-tongued bees are defined by a glossa that is longer than the mentum and generally with the labial palpomeres similar to one another, whereas the mentum is longer in the long-tongued bees which have the first two labial palpomeres much longer than the apical two which are at right angle to the first two. In the total of seven recognized bee families, five are short-tongued: Colletidae, Stenotritidae, Halictidae, Andrenidae, Mellitidae; and two are long-tongued: Apidae and Megachilidae (Michener 2007). For most of the history of bee classification, mouthparts served as evidence of early ancestry of the Colletidae, marked by its bifid wasp-like glossa (Engel 2001). This notion formed the classical view of bee evolution in which the bifid glossa was thought to be homologous with that of the apoid wasps (Michener 1944).

While some phylogenies derived from morphological data suggest antiquity of Colletidae (Alexander and Michener 1995), more recently, molecular data rather consistently hypothesizes Melittidae as being the earliest bee lineage, which renders Colletidae as a more derived family

(Danforth et al. 2006, Brady et al. 2011, Debevec et al. 2012, Hedtke 2013, Branstetter et al. 2016).

Since almost all bees are entirely dependent on angiosperms for their food source (pollen, nectar and sometimes oil), it is thought they have either coevolved with or arose after angiosperms which originally were primarily pollinated by beetles (Grimaldi 1999, Cardinal and Danforth 2013). Angiosperm biogeography studies reveal that by the end of the Cretaceous angiosperm diversity had increased to such extent that their pollination was likely aided by bees. Some forms present at that time (e.g. Myrtaceae) are in families and genera that are now primarily pollinated by bees (Cardinal and Danforth 2013). More recently, there has been evidence of an earlier rise of bees, dating to the late Lower Cretaceous and coinciding with the diversification of eudicots (Engel and Rightmyer 1996, Engel 2001, Michener 2007, Cardinal and Danforth 2013).

The fossil record of bees is generally scarce and mostly limited to the Tertiary period, with most of the material covering Eocene and Miocene epochs (Michez et al. 2012), with a couple of recent fossil discoveries that date back to the early to late Cretaceous. One of these is a meliponine bee preserved in the Maastrichtian-aged Raritan amber, phylogenetic analysis of which suggests that the tribe of the fossil dates to at least the late Cretaceous (Michener and Grimaldi 1988, Cardinal and Packer 2007, Dehon et al. 2014). Whereas the other – more recent discovery of a new bee family, Melittosphecidae, in Burmese amber, has set a new minimum date for antiquity of bees to the early Cretaceous (Poinar and Danforth, 2006). Ohl and Engel (2007) argued this, suggesting that the specimen might be a predatory wasp, whereas Danforth and Poinar (2011) identify it as a transitional specimen relating closer to bees and linking bees with crabronid wasps.

Unlike trilobites, for which there is an impressive fossil record, representation of antique bees and insects in general contains many gaps (Michez et al. 2012). Even within Apoidea the fossil record is inconsistent among families and is biased towards certain groups. To date, there is fossil evidence for five bee families: Apidae, Megachilidae, Andrenidae, Haclictidae and most recently, Colletidae (Engel 2001, Poinar and Danforth 2006, Michez et al. 2008, Michez et al. 2012, Dehon et al. 2014, Dehon et al. 2017). In addition to geographical distribution of bees, feeding and nesting habits play a crucial role in the likelihood of an animal being preserved. Resin-collecting corbiculate bees (Apidae), for example, have an impressive representation in amber fossils, 61% of all described bee fossils belong to this group (Michez et al. 2012). Conversely, the likelihood of stem-nesting bees, such as some Colletidae, being preserved in carbonaceous film (carbon residue imprint of the fossil on the rock) or amber is low. Hence, the improbable discovery of the first two *C. (Hylaeosoma)* (Colletidae) amber fossils (Engel 1999) gave ground for exciting and novel study opportunities for the study of Colletidae and bees in general.

Apart from helping infer phylogenetic relationships, fossils are useful in extracting other essential information. Until recent developments in molecular phylogenetics and other analytical methods, fossils were used in determining the direction of character change and in detecting instances of convergence (Hennig 1966, Engel 2001). Now, in combination with molecular data, fossils are used to calibrate phylogenetic timelines produced by molecular data (Danforth et al. 2006). However, molecular phylogenies alone are only capable of providing relative timelines computed by Bayesian statistical models. It is the fossils that can place an absolute date on those timelines and calibrate the phylogeny accordingly (Donoghue et al. 1989).

Despite the recent exponential growth in the ability to acquire vast amounts of DNA to infer phylogenies from genome-scale datasets, traditional morphological phylogenetic methods remain essential for integrating fossils into phylogenetic analyses to estimate the timing of evolutionary events (Dunn et al. 2008). For this reason, morphological data allows for integration of extinct taxa into trees along with the living taxa, uncovering past diversification events generally inaccessible to genomics (Dunn et al. 2008). Even though phylogenomics generate trees that are fully resolved and well-supported, and arguably are viewed as the most powerful and efficient ways of constructing evolutionary trees for living organisms, it is the combined molecular and morphological information of extant and living taxa that is necessary for a comprehensive understanding of evolution (Donoghue et al. 1989).

Multiple methods have been developed that use combined molecular data with morphological and/or temporal data of fossils to transform undated molecular tree topologies into dated evolutionary trees. The three methods are node-dating, tip-dating and birth-death ratio (Arcila et al. 2015, Ronquist e al. 2012, Heath et al. 2014). The methods vary by the number of fossils than can be used and the extent of fossil integration into the analyses, ranging from extrapolation of only the age of the fossil, to incorporating morphological data to infer the placement of the fossil in the phylogeny and simultaneously calibrating all the nodes in the tree (Arcila et al. 2015, Pyron 2011, Ronquist e al. 2012, Heath et al. 2014). All of the above methods are still used to accommodate the differences in available information and study designs. For example, Praz and Packer (2014) used node-dating to produce a dated phylogeny for the Eucerini and related tribes, this was the preferred method because the generic or tribal placement of the only available eucerine fossil could not be confirmed.

Grimaldi (1999) summarized numerous studies that demonstrated successful estimation of date ranges for nodes of various insect groups by incorporating fossil taxa into phylogenetic analyses. He focused on studies examining phylogenetic relationships of early pollinators such as some Hymenoptera (Apoidea) and most Diptera and Lepidoptera – concluding early to mid-Cretaceous, upper Jurrassic and lower to mid-Jurrassic origins, respectively. An earlier study using modern molecular clock dating methods to determinate origins of various insect groups arrived at a similar conclusion for Lepidoptera, but estimated an earlier date for Diptera, affected by the discovery of a Central Asian Triassic dipteran (Shcherbakov 1995), with which molecular data still accords (Gount and Miles 2002). Another study incorporating fossil and molecular data of halictids arrived at a similar conclusion of bee divergence in the Cretaceous (Danforth et al. 2004).

As previously noted, some fossils are preserved in ways that limit the number of visible or accessible characters - providing insufficient evidence for forming well-supported phylogenetic relationships. This is especially an issue with carbonaceous films - where usually only a partial two-dimensional imprint of an animal is available, and is less so with inclusion fossils, such as in chert, onyx, gypsum and amber – where generally an entire animal or a portion of one is preserved in three dimensions. One of the solutions for maximizing the phylogenetic data from such fossils is to use geometric morphometrics. This approach uses information on spatial covariation among landmarks (Rohlf and Marcus 1993). Geometric morphometrics is especially practical for wing venation characters, as for the most part, these are well preserved in fossils and provide easily distinguishable two-dimensional landmarks at vein interceptions and terminations. Combination of qualitative morphological characters, which are usually limited in fossils, and

quantitative morphometrics data, can collectively provide sufficient evidence for the fossil taxa to be used to infer dated phylogenies (Eernisse and Kluge 1993).

Only recently have *C. (Hylaeosoma)* fossils been incorporated into studies looking at Colletidae evolution, and were only utilized for node-dating (assigning minimum age to the node based on the age of a single fossil) (Almeida et al. 2011, Cardinal and Danforth 2013, Kayaalp et al. 2017). One of these studies looked at Colletidae biogeography and diversification rates of the family (Almeida et al. 2011). Integration of fossils in this study was imprecise for two reasons: first, the lack of *C. (Hylaeosoma)* DNA complimenting the fossil evidence; and second, the lack of the placement of fossils within the phylogeny; both needed for a comprehensive, precise calibration of the tree. This thesis serves to correct the second issue by placing fossils within the phylogenetic tree along with extant taxa.

*Chilicola* Spinola, 1851 is a diverse neotropic genus of small, 3-9 mm long, hylaeiform, stem-nesting bees (Michener 2007). The genus consists of 105 species (Ascher and Pickering 2016), classified into 15 subgenera (Packer 2008), with the most recent addition of seven new species from Chile (Monckton 2016). The subgenus *Chilicola (Hylaeosoma)* Ashmead, 1900 consists of 19 described species, plus an additional 7 described herein, ranging from northeastern Mexico to southern Peru, and is the only subgenus of *Chilicola* to inhabit the Caribbean. Notably, *C. (Hylaeosoma)* contains the only two fossils known for its family - Colletidae, preserved in Oligo-Miocene Dominican Amber (15-20 Ma; Michener and Poinar 1996, Engel 1999). *Chilicola (Hylaeosoma)* was originally described as a genus based upon *H. longiceps* Ashmead, 1900 from Saint Vincent and the Grenadines, and only comparatively recently recognized as belonging within *Chilicola* by Michener (1995).

The species of *C. (Hylaeosoma)* have unusually slender bodies, 4.5 to 8.0 mm long, and for most part lack yellow markings or only show yellow on basal and apical tarsal extremities or on the clypeus of the males (Michener, 2007). It can be differentiated from other *Chilicola* by the stigma extending beyond the apex of the second submarginal cell and an elongate lateral intercoxal area not associated with a strongly modified hind leg (Packer, 2008). *C. (Hylaeosoma)* is generally subdivided into two species groups based on morphology: the *longiceps* and *megalostigma* species groups (Michener, 2002). Members of the *longiceps* group lack a preoccipital carina, have more-or-less round heads and dull integument. The *megalostigma* group contains bees with elongate heads, a strong preoccipital carina and shiny integument; they are also generally more slender than bees of the *longiceps* group. All of the defining characteristics of the *megalostigma* group are apomorphic in relation to the contrasting states of the *longiceps* group, suggesting the possibility that the latter is paraphyletic (Michener 2002). Many species of *Chilicola,* including *C. (Hylaeosoma),* build their nests in pithy stems (Benoist 1942), while some nest exclusively in wood or in wood stem burrows previously made by beetles (Michener 2002).

To date, no species-level revisionary work has been done on the subgenus, leaving a collection of unidentified specimens recognized as *C. (Hylaeosoma).* Additionally, no phylogenetic work has been done that incorporated the fossils. Here, I will describe seven new species of *C. (Hylaeosoma)* and conduct a phylogenetic analysis including fossil taxa - necessary for more accurate node-dating and essential for time-calibration of larger data sets (Danforth et al. 2006, Almeida et al. 2011, Hedtke et al. 2013).

Owing to the nature of fossil preservation, only a limited number of characters are visible, and traditional discrete morphological characters may not be sufficient to place the fossil into the

tree robustly. However, because wing venation is usually well preserved in fossils, it can be useful in understanding insect evolution. While shape information, known as geometric morphometrics, has repeatedly produced stronger phylogenetic signals when compared to other characters (Bai et al., 2013; Perrard et al., 2016), its use in phylogenetic analyses has been a subject of long debate (Bookstein, 1994; Rohlf, 1998; Gonzalez-Jose et al., 2008; Catalano et al., 2010). Because shape data are continuous they have not been compatible with traditional phylogenetic analytical frameworks (Bookstein, 1994). However, the development of a new "landmark analysis under parsimony" (LAUP) method and its implementation in TNT has been able to resolve this issue (Goloboff et al. 2006, Catalano et al. 2010, Goloboff and Catalano 2016) and prompt its use in recent studies (Perrard et al. 2016, Roggero et al. 2016, Catalano et al. 2017). This method, just as in standard parsimony analysis, maximizes the degree to which similarity in landmark position among taxa can be regarded as common ancestry (Catalano et al. 2010). For this study's purpose, this method shows significant promise for placing *C. (Hylaeosoma)* fossils within the phylogeny.

## MATERIALS AND METHODS

### *Taxonomy*

The extant and amber fossil bee specimens for examination were obtained from multiple collections, listed in Table 1. Specimens were identified using keys (Michener 1992, Michener 2002, Gonzales and Giraldo 2009, de Oliviera et al. 2011, and Packer, 2008 for subgenus identifications) and those not matching any descriptions of the species were sorted into operational taxonomic units. Prior to confirmation of these specimens as undescribed species, where possible, they were compared to holotypes, and when these were unavailable, to paratypes of existing species.

New descriptions were based on the format and terminology of Michener (1995 and 2002), who contributed the most to species descriptions of the subgenus, with the exception of *metapostnotum* used to describe the "dorsal surface of the propodeum" (Brothers 1976).

Body measurements were taken using a calibrated ocular micrometer mounted on a Nikon SMZ1000 microscope. Measurements were recorded in millimeters (mm). Total body length was measured in sections (head, meso- and metasoma) and summed. All other relative body measurements were expressed as ratios. The following abbreviations are used: UOD – upper interocular distance, LOD – lower interocular distance, MOD – median ocellus diameter (primarily used as a reference measurement in describing the length of pubescence), T – metasoma terga, S – metasomal sterna, and F – antennal flagellomeres.

All images were taken using a Visionary Digital lift-operated imaging system and a Canon 5D Mark II digital SLR camera. Composite images were amalgamated using Zerene Stacker software. All other image processing was performed in Adobe Photoshop CS6 Extended ver. 13.0.

### *Phylogenetic analysis*

Phylogenetic relationships were inferred for sixteen extant and two fossil species of *C. (Hylaeosoma).* The following five taxa from four additional subgenera were selected as outgroups based on the findings of Packer (2008): *C. (Unicarinicola) unicarinata* Packer 2007, *C. (Pseudiscelis) rostrata* (Friese, 1906), *C. (Pseudiscelis) nanula* Packer, 2007, *C. (Prosopoides) prosopoides* (Ducke, 1907), *C. (Prosopoides) granulosa* Packer, 2007. Two sister subgenera *Prosopoides* and *Pseudescelis* were chosen to represent the sister clade of *C.*

*(Hylaeosoma). Unicarinicola* was chosen to root the tree as it forms the sister group to the other three subgenera combined (Packer, 2008).

A total of 96 morphological characters were coded for each species – 92 discrete and 4 continuous shape configurations, of which 89 discrete phylogenetically informative characters were adapted from Packer's phylogenetic analysis of Xeromelissinae (2008). Forty-seven and nineteen discrete morphological characters were scored from fossils of *C. electrodominica* and *C. gracilis,* respectively. Characters of *C. gracilis* were obtained solely from its description (Michener and Poinar 1996), whereas *C. electrodominica* was scored from the fossil holotype. All discrete characters were entered into Mesquite version 1.3(Maddison and Maddison 2001), while landmark coordinates were saved as separate text files. The majority of discrete characters were taken from males, on the basis of larger variation in secondary sexual characteristics. Female characters that were similar to those of males were assessed to ensure they were independent and not confounded between the sexes.

Phylogenetic analysis of combined landmark and discrete character data was done using landmark analysis under parsimony (LAUP) implemented in TNT version 1.5 (Goloboff and Catalano 2016). This version includes a full integration of landmark data for the analyses. Analytical settings were set to default, except as noted below. Ratchet, drift and tree fusing set to ten was used to find the most parsimonious tree. Successive approximations character weighting was performed using the rescaled consistency index as the weighting factor. Implied weight analysis employed setk.run script to find the concavity function and generate a FIT measure to find the best tree. Symmetrical resampling (Goloboff et al. 2003) was performed on unweighted results with 500 iterations. This relatively low iteration number was used due to computationally intensive process for analyzing landmark data.  Support for the nodes was expressed in GC

values representing a ratio of the frequency of the group versus the most commonly found contradictory topology. Additionally, bootstrap values were calculated using default TNT settings and 500 iterations. Identical analyses were performed for discrete morphological characters alone, except with 10 000 iterations for symmetrical resampling and bootstrap analyses.

### *Geometric morphometrics*

The right wings of 35 specimens were measured for 19 species of *C. (Hylaeosoma)* and one outgroup species (Table 1). Only females were measured to avoid potential biases linked with sexual dimorphism as well as missing data associated with fewer species available from males than females. Wings were removed from specimens and placed on a slide for imaging by the system described above. The image file was prepared for digitizing the landmarks in tpsUtil ver. 1.44 (Rohlf 2009). A total of 26 landmarks for four configurations were digitized using tpsDig2 software (Rohlf 2010, Figure 1). The four configurations were selected to represent non-overlapping wing venation characters, denoted as C1, C2, C3, C4 for configurations 1, 2, 3 and 4, respectively. C1 encompasses the radial cell, C2 represents the stigma and marginal cell, C3 encompasses the second medial cell, and C4 represents the posterior margin of the second cubital cell.

To remove all information unrelated to shape, such as size, position and scale, a generalized least-squares Procrustes superimposition (Rohlf and Slice 1990) was conducted in CoordGen ver. 7A (Sheets 2003a). The mean wing shape was computed using RFTRA superimposition for the aligned coordinates of each species (Catalano et al. 2010).

To test for independence among configurations, a level of association (RV score) was calculated using Partial Least Squares (PLS) analysis with 1000 permutations in MorphoJ (Klingenberg 2011). The analysis was done on individual specimens as well as pooled within species to remove any influence from intraspecific association. A principal component analysis (PCA) was used to visualize total maximum amount and direction of wing variation. A canonical variate analysis (CVA) was performed to test the taxonomic signal of wing shape in CVAGen ver.8 (Sheets, 2003b), with a Jackknife grouping test (Webster and Sheets, 2010). This test works by assigning specimens into groups ignoring *a priori* established grouping and the percentage of specimens placed into the correct group is then calculated. Because the number of landmarks is higher than the number of specimens per species, a Jackknife test for species groupings had to be performed on PCA scores (cumulative eigenvalues above 95%) as opposed to original landmark coordinates (Webster and Sheets, 2010). Morphogroups, on the other hand, containing larger sample size per group, were analyzed from Procrustes aligned coordinates. A MANOVA test of significance was included in the CVA to test for size and significance of variation of wing shape configurations among species.

Phylogenetic signal was tested by mapping shape information (PC scores) onto the discrete morphological phylogeny in MorphoJ and performing a permutation test (10 000 randomization rounds) against the null hypothesis of no phylogenetic signal.

**Table 1:** List of species measured for forewing shape. *N*, sample size. Museum abbreviation are as following PCYU (Packer Collection at York University), AMNH (American Museum of Natural History), KU (Kansas University) Biodiversity Institute, USDA (United States Department of Agriculture).

| **Name** | ***N*** | **Museum** |
|---|---|---|
| *Chilicola prosopoides* (Ducke, 1907) | 1 | PCYU |
| *Chilicola aequatoriensis* Benoist, 1942 | 3 | AMNH, KU, USDA |
| *Chilicola belli* Michener, 2002 | 2 | KU |
| *Chilicola involuta* Michener, 2002 | 3 | KU |
| *Chilicola longiceps* (Ashmead, 1900) | 1 | KU |
| *Chilicola megalostigma* (Ducke, 1908) | 3 | KU, USDA |
| *Chilicola mexicana* Toro and Michener, 1975 | 2 | KU, USDA |
| *Chilicola polita* Michener, 1994 | 2 | AMNH, KU |
| *Chilicola smithpardoi* Michener, 2002 | 2 | PCYU |
| *Chilicola herberti* Miklasevskaja, 2017 | 1 | PCYU |
| *Chilicola rufotergata* Miklasevskaja, 2017 | 1 | PCYU |
| *Chilicola paveli* Miklasevskaja, 2017 | 2 | PCYU |
| *Chilicola liudmilae* Miklasevskaja, 2017 | 3 | USDA |
| *Chilicola boyacense* Miklasevskaja, 2017 | 4 | PCYU |
| *Chilicola boliviana* Miklasevskaja, 2017 | 1 | USDA |
| *Chilicola lambayequense* Miklasevskaja, 2017 | 1 | PCYU |
| *Chilicola yanezae* Hinojosa-Díaz and Michener, 2005 | 1 | KU |
| *Chilicola gracilis* Michener & Poinar 1996 | 1 | AMNH |

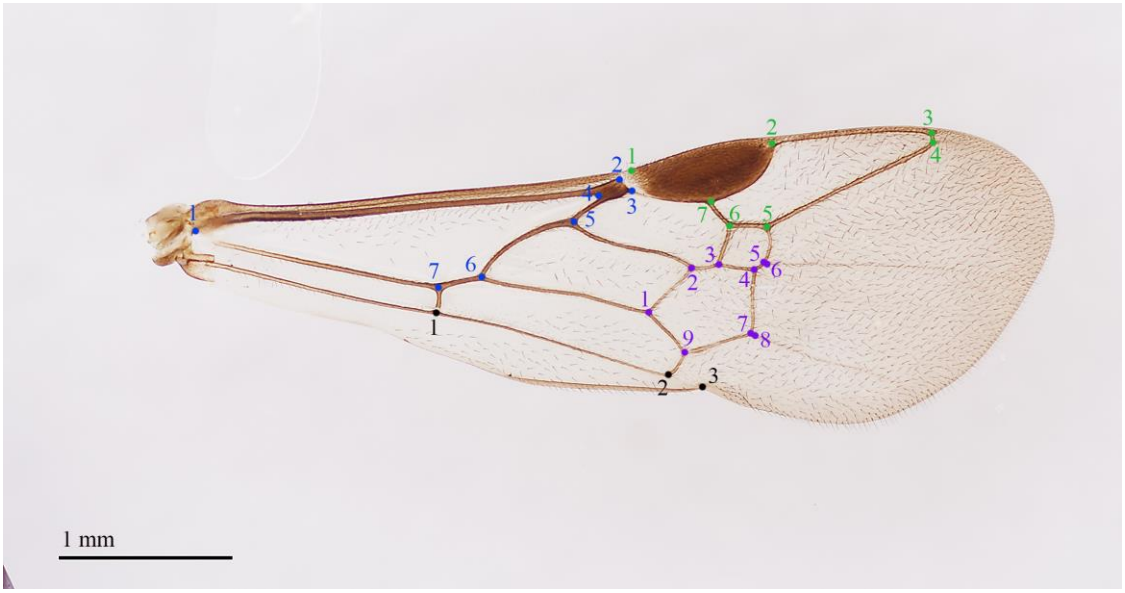


**Figure 1:** Image of forewing of *C. megalostigma* to display wing landmarks. Circles indicate the location of 26 landmarks. Blue, green, purple and black colours are used to differentiate configurations 1-4, respectively.

## Results

*Taxonomy*

**Genus *Chilicola* Spinola Subgenus *C. (Hylaeosoma)* Ashmead**

***Chilicola* (*Hylaeosoma*) *herberti* Miklasevskaja**

**Holotype.** ♂, Brazil, Vicosa (14.II.2005 [14 February 2005], C.A. Silva *Leg.* // Colletidae: *Chilicola* (*Hylaeosoma*) sp. N., Det. Miklasevskaja, 2015 // Collected on flower: Rubiaceae: *Psychotria hastisepala* Müller Argoviensis. The metasoma is separated from the specimen, otherwise it is in an excellent condition and is currently deposited in the Packer Collection at York University (PCYU) in Toronto, Ontario, Canada.

**Allotype.** ♀, with same label data as holotype. PCYU.

**Diagnosis.** Both sexes of *C. herberti* can be differentiated from all others in the subgenus by the shape of the head, which is almost twice as long as wide. All other species have the head at most 1.5X as long as wide with the exception of *C. kevani* which in the male (the female is unknown) has the head more than 2X as long as wide. For the female, the extensive honey yellow of the mesosoma and T1 are also unique for the subgenus although it is possible that the unknown female of *C. kevani* might also be extensively pale.

**Description.** ♂: *Structure*: Body length 9.30 mm; forewing length 5.40 mm; intertegular width 1.1 mm. Head elongate (Fig. 2A), length 2.25 mm, width 1.30 mm; compound eyes strongly converging below, upper ocular distance (UOD) 0.73 mm, lower ocular distance (LOD) 0.27 mm; paraocular area with a weak depression for reception of scape, terminating at level of upper tangent of compound eyes and curved around a prominent grey oval spot 1.5MOD in

diameter and 1.86×longer than broad; frontal line with conspicuous depression 1MOD broad just above level of antennal sockets; F1 slightly longer than pedicel and 2× longer than broad; F2 and F3 as long as broad; F11 approximately 3× longer than broad; malar area 1.5× broader than long; ocelloccipital distance about 1.8MOD as measured from apex of preoccipital carina; preoccipital carina laminate (Fig 2B); T1 ~1.5X longer than broad, length 1.23 mm, width 0.83 mm; T2 and T3 weakly depressed in basal half in profile; distal margin of S6 terminating in two lateral lamellate projections; S7, S8, and genitalia as in figure 3: S7 ventral lobe somewhat diamond shaped with medial margin convex, lateral margin weakly sinuate, with posterior and lateral margins converging to narrowly pointed apex, comb of long (some branched) setae with sharply curved apices along posterior margin, minute simple setae on posterior half of dorsal surface, dense medially; S7 dorsal lobe reduced to small process; S8 apical process elongate quadrifurcate with simple long setae between basal and apical processes; genital capsule as in figure 3, with gonostylus narrowly rounded apically and curved ventrally near apex.

*Sculpturing*: Integument polished and shining, smooth or with very faint microsculpture; scattered shallow punctures throughout, most punctures separated by more than 2–3× a puncture width; two small, kidney-shaped foveae near concavity of compound eyes; metapostnotum with approximately 22 longitudinal carinae radiating towards apex.

*Coloration*: Integument predominantly dark brown except as follows (Figs. 2A,B): labiomaxillary complex, scape, and pedicel honey yellow; F1 lighter brown than remainder of flagellum; pronotal lobe honey yellow; mesoscutellum, tegula translucent, honey yellow; axillary sclerites brown, base of M+Cu and V honey yellow, pterostigma brown; hind wing venation honey yellow, except R dark brown; wing membrane hyaline, slightly and faintly infumate apically; mesal legs honey yellow with outer surface of mesofemur slightly darker; hind coxa

and trochanter honey yellow; apical margin of T2, T3, T5 and all of T6 light brown: S3 with lighter brown apical band and lighter medial area on S4 and S5; S6 light brown.

*Pubescence*: Mostly golden; head with scattered, largely simple setae, 1.5-2 MOD in length, those on supraclypeal, frontal, vertexal and hypostomal areas longer; a few short, branched setae on face near concavity of compound eyes. Mesosomal setae short and simple, posterior margin of pronotum and lateral margins of mesoscutum with numerous, minute, pale, branched setae, becoming paler around pronotal lobe; mesoscutum with short and sparse setae; mesoscutelum and metanotum with relatively long setae, 1.5-3MOD, longer setae apically curved; metapleuron and lateral surface of propodeum with relatively short, dense setae; mesopleuron with long, scattered simple setae, less numerous on mesepisternum, setae of prepisternum slightly denser, shorter hairs around the posterior margin; procoxa, protrochanter and ventral surface of profemur with dense, long branched setae; metacoxa, metatrochanter and ventral surface of metafemur with sparse, long, simple setae; setae shorter on outer surfaces of metatibia and metabasitarsus. Metasoma with sparse, long setae, progressively longer on more apical segments; apicolateral margins of S2-S5 with very long, thick setae, curving apicomedially on S4 and S5; S6 with an apical patch of several short lateral setae and a row of long medially directed setae curved at apex.


**Figure 2:** Images of *C. herberti.* Top, male; bottom, female.

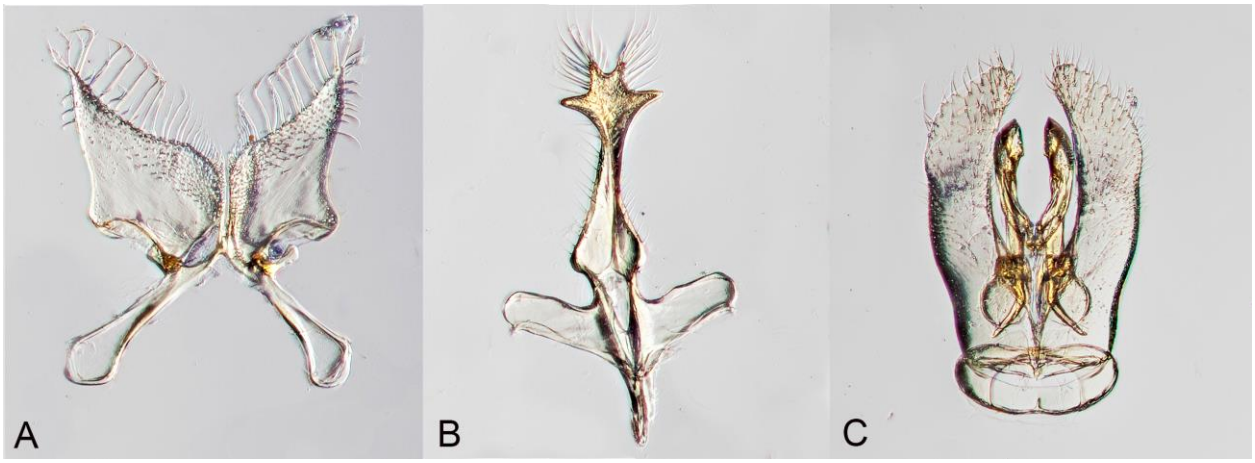


**Figure 3:** Terminalia of *C. herberti.* A, S7; B, S8; and C, genital capsule.

♀: As in male except for usual secondary sexual characters and as follows: *Structure:* Body length 7.60mm; forewing length 6.10mm; head width 1.10 mm; head length 2.05 mm, LOD 0.37 mm; gray oval spot absent; frontal line depression smaller, 0.25MOD in length; F2 and F7-F9 as long as broad; F3-F5 1.5× broader than long; F10 approximately 2× longer than broad; malar area 2× broader than long; metasomal T1 as long broad; T2 weakly depressed in basal half in profile.

*Sculpture:* Metapostnoutm with approximately 17 longitudinal carinae set in slight depression and radiating from basal margin.

*Coloration*: Integument predominantly honey yellow (Figs. 2C,D); head dark brown except labiomaxillary complex and scape honey yellow; anterior portion on clypeus light brown; F1-F10 dark brown; entire thorax and T1 honey yellow; base of C, M+Cu and V honey yellow, otherwise forewing venation brown, pterostigma brown; legs honey yellow except mesobasitarsus, mesomediotarsi, base of metafemur, metatibia and metatarsus dark brown; abdominal terga dark brown except T1and base plus apical margin of T2 honey yellow; sterna dark brown except S1 and most of S2 honey yellow.

*Pubescence*: Mesosomal setae generally simple except plumose around pronotal lobe; posterior margin of pronotum and lateral margins of mesoscutum with numerous, minute, pale, branched setae; meso- and metacoxae, meso- and metatrochanter with dense, long (0.5× length of scape ) branched setae; metasoma generally with sparsely scattered setae, setae becoming progressively longer and denser on more apical terga; long plumose setae on S1-S3, mix of simple and branched setae on S4, simple, short dense hairs on apical margin of S5 and S6.

**Etymology:** Named after Frank Herbert, an author of science fiction novels, for close resemblance of male terminalia to fictional spaceships. It is formed in the genitive singular case.

***Chilicola* (*Hylaeosoma*) *rufotergata* Miklasevskaja**

**Holotype.** ♂, Peru, Ayacucho (3.IV.2010 [3 April, 2010], Packer/Rivera. Colletidae: *Chilicola* (*Hylaeosoma*) sp. N., Det. Miklasevskaja, 2015. Specimen is missing a right hind leg, otherwise in excellent condition and is currently deposited in the Packer Collection at York University (PCYU) in Toronto, Ontario, Canada.

**Allotype.** ♀, with same label data as holotype, except for the date (2.IV.2010 [2 April, 2010]). The female specimen is missing a right hind leg, otherwise in excellent condition and is deposited in the same collection as the holotype.

**Diagnosis.** Males of this species differ from all other members of the subgenus in that it has a white medial mark on the clypeus and a distinct pale mark at the base of the hind tibia. All other species lack such pale colouration. The modifications of S4 and S5 are also unique to *C. rufotergata*, its S4 has two mid-lateral swellings each with a pit at the summit, and S5 has a medial, prism-shaped lamellate process; all other species in the subgenus lack modifications to these sterna. Females can be differentiated from other members of the subgenus by having a red/brown T1-T3, the only other species with pale markings on the metasoma is *C. herberti* which also has a pale mesosoma and with pale metasomal markings restricted to T1.

**Description.** ♂: *Structure*: Body length 3.87 mm; forewing length 3.00 mm, intertegular distance 0.7 mm. Head slightly elongate (Fig. 4A), length 1.19 mm, width 0.88 mm; UOD 0.56 mm, LOD 0.39 mm; paraocular area deeply impressed for reception of scape, depression

terminating at level of upper tangent of compound eye; pedicel as broad as and more than half as long as scape; 10 flagellomeres total; F1 slightly shorter than pedicel and 2× longer than broad; F4 as long as broad; malar area linear; occeloccipital distance 1MOD as measured from margin of the sharply rounded preoccipital ridge; T1 length and breadth subequal (0.85mm: 0.80mm respectively); S4 with two mid-lateral swellings each with a pit at the summit; S5 with a medial, prism-shaped lamellate process. S7, S8, and genitalia as in figure 3: S7 ventral lobe elongate, laterally directed and acutely pointed, with apical patch of short hairs and a basal row of long hairs; S7 dorsal lobe almost forming an equilateral triangle with posterior corner curved; genital capsule as in figures 5C, with flattened membranous gonostylus curved ventrally near apex; mesoventral lobe swollen and anteromedially directed; penis valves with membranous lobes.

*Sculpturing*: Integument mostly dull and coarsely microsculptured (as in other species of the *longiceps* group); mesoscutum, scutellum with punctures separated by at most one puncture diameter except sparse towards sides of mesoscutum; impunctate, shiny fovea mesad of concavity of compound eye, marked by lateral carina; metapostnotum rugose anteriorly with faint median carina.

*Coloration*: Integument predominantly black (Fig. 4A, B); head black except yellow longitudinal mark on clypeus, entirely yellow mandible and brown labiomaxillary complex; tegula translucent, testaceous; forewing venation brown, pterostigma brown; hind wing venation light brown, except dark brown Rs; wing membrane infumate; preepisternum, mesepisternum and metepisternum black; legs predominantly dark brown except apical margin of femora, apex of all tibiae honey yellow, tarsi light brown; metasoma dark brown except base of T2 and T3 honey brown and apical margin of T1-T4 transluscent; S6 honey brown.

*Pubescence*: Mostly white; head with scattered, minute largely simple setae, <1MOD in length, except on supraclypeal, frontal, vertexal and hypostomal areas branched and longer, 1.5-2MOD in length. Mesosomal setae relatively long and branched, except more minute around pronotal lobe; mesoscutum and mesoscutelum with relatively short and sparse setae; pronotum with dense, simple, short setae; metanotum with relatively long setae, 1.5-2MOD, curved medially; meso- and metapleuron with sparsely scattered, short, branched setae; lateral surface of propodeum with simple minute setae all over, except longer and branched setae dorsally; ventral surface of pro- and metacoxa, pro- and metatrochanter, pro- and metafemur and metabasitarsus with relatively long, branched setae, 1MOD in length; Metasoma with minute setae throughout, denser and longer on lateral apical margins of terga and progressively longer towards apex; sterna with visibly longer setae; setae on S1 long and plumose, 2-3MOD in length, S2-S6 with long branched setae, 1-2MOD in length.

♀: As in male except for usual secondary sexual character and as follows: *Structure*: Body length 4.83 mm, forewing length 3.2 mm. Head length 1.27 mm, width 0.95 mm; UOD 0.70 mm, LOD 0.45 mm; F2 and F3 as long as broad; F4-F9 broader than long.

*Coloration*: Integument predominantly black (Fig. 4C, D); head black except brown labiomaxillary complex, and honey brown apical half of mandible and posterior of F6-F10; preepisternum, mesepisternum and metepisternum black; legs predominantly dark brown except basal margin of tibia pale yellow, tarsi dark brown; abdominal terga red-brown except base of T1, T4-T6 brown; S2–S3 honey brown; S1, S4-S6 dark brown.

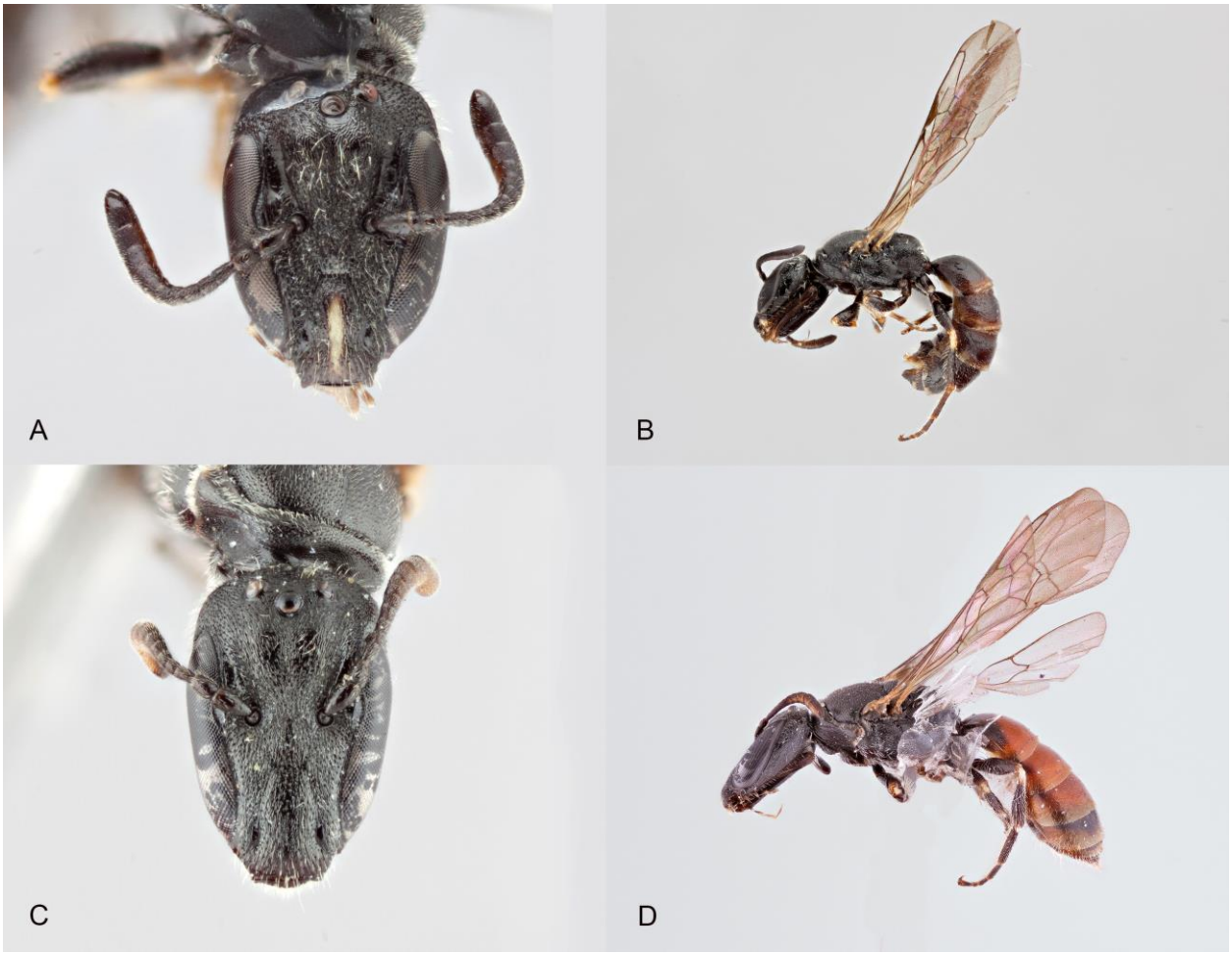


**Figure 4:** *Chilicola rufotergata.* Top, male; bottom, female.

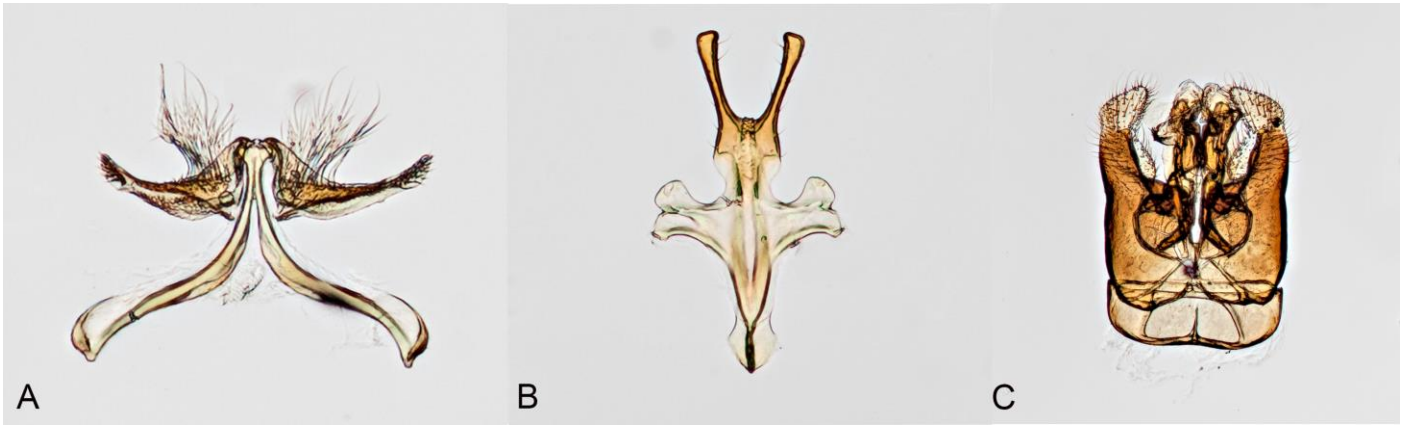


**Figure 5:** Terminalia of *C. rufotergata.* A, S7; B, S8; C, Genital capsule.

*Pubescence*: Mostly white; head with scattered, minute, largely simple setae, <1MOD in length, except longer on supraclypeal, fronal, vertexal and hypostomal areas. Metanotum with long setae, longer and branched near lateral margin, 1.5-2MOD in length, curved medially. Metasoma with minute setae throughout, denser and longer on lateral apical margins of terga and progressively longer towards apex; sterna with visibly longer setae; S1 with few long plumose setae, 2-3MOD in length; S2 with setae as S1 but denser; S3 with long branched setae; S4-S6 with long simple setae.

**Etymology:** From Latin *rufo* (an adjective of *rufus*), and *terga* to denote the red metasomal terga of the female.

***Chilicola* (*Hylaeosoma*) *paveli* Miklasevskaja**

**Holotype.** ♂, Peru, Cuzco (21-24.X.1972 [21-24 October, 1972], P. Wygodzinsky. Colletidae: *Chilicola* (*Hylaeosoma*) sp. N., Det. Miklasevskaja, 2016. Specimen is in excellent condition and is deposited in the Packer Collection at York University (PCYU) in Toronto, Ontario, Canada.

**Paratypes:** Four males with the same locality and date information as the holotype.

**Diagnosis.** This species can be differentiated from all others by its wide head with length at most 0.9X its width. *Chilicola aequatoriensis* possess a similarly round head shape however it is at least 1.05X longer than wide. In addition, *C. paveli* can be distinguished from *C. aequatoriensis* by its more densely punctured mesoscutum, with punctures separated by 1MOD or more, as opposed to 2MOD or more in *C. aequatoriensis.* Additionally, it can be easily differentiated by its unique hidden sterna (Fig 7).

**Description.** ♂: *Structure*: Body length 5.54 mm; forewing length 3.85 mm, intertegular distance 0.86 mm. Head appearing almost round (Fig. 6A, B), length 0.98 mm, width 1.05 mm; UOD 0.84 mm, LOD 0.50 mm; paraocular area somewhat impressed for reception of scape, depression terminating below level of upper tangent of compound eye; pedicel less broad and less than half as long as scape; F1 about as long as pedicel and almost as long as broad; F2 and F3 broader than long; F4 as long as broad; malar area linear; occeloccipital distance 1MOD as measured from margin of the sharply rounded preoccipital ridge; T1 1.36 times longer than broad (0.75mm: 0.55mm respectively); S2 with two mid-lateral swellings; S7, S8, and genitalia as in figure 7: S7 ventral lobe kidney shaped and laterally directed, with long curved bristles on an apical patch and long simple bristled on an anterior margin; S7 dorsal lobe digitiform and laterally directed with a tuft of short curved setae on its lateral margin (Fig. 7A); genital capsule as in figure 7B, with flattened gonostylus slightly curved ventrally near apex; mesoventral lobe swollen and anteromedially directed.

*Sculpturing*: Integument mostly dull and coarsely microsculptured (as in other species of the *longiceps* group); mesoscutum, scutellum, metanotum with punctures separated by equal or less than one puncture diameter except sparser mid-laterally of mesoscutum; mesepisternum lineolate with sparsely scattered punctures situated between ridges; impunctate, shiny fovea mesad of concavity of compound eye, marked by lateral carina; metapostnotum with many fine striae and faint median carina.

*Coloration*: Integument predominantly black (Fig. 6A, B); head black except brown apex of mandible and light brown labiomaxillary complex; tegula translucent, testaceous; forewing venation brown, pterostigma brown; hind wing venation light brown; wing membrane infumate;

preepisternum, mesepisternum and metepisternum black; legs dark brown; metasomal terga brown, sterna light brown.

*Pubescence*: Mostly white; head with scattered, minute largely simple setae, <1MOD in length, except on clypeal, supraclypeal, vertexal and preoccipital areas longer, 1-1.5MOD in length. Hypostoma with long (1.5MOD) branched setae. Mesosomal setae relatively long and branched, except more minute around pronotal lobe; mesoscutum and mesoscutelum with relatively short and sparse setae; pronotum with realtively dense, simple, short setae; metanotum with relatively short scattered setae, 0.5MOD; meso- and metapleuron with sparsely scattered, short, branched setae (1MOD); lateral surface of propodeum with largely simple minute setae all over, except for longer and branched setae scattered sparsely throughout; dorsal surface of pro- and metafemur, with relatively long, branched setae, 1MOD in length, otherwise legs with simple minute hairs. Metasoma with minute setae throughout, longer on lateral apical margins of terga and progressively longer towards apex; sterna with visibly longer setae; setae on S1 and S2 long and branched, ~2MOD in length, S3-S6 with shorter branched setae, 1-1.5MOD in length.

**Etymology:** In honour of Pavel Fedotov, whose ongoing support and encouragement kept me on track to complete this project. It is formed in genitive singular case.


**Figure 6:** *Chilicola paveli* (A, B) and *C. liudmilae* (C, D).

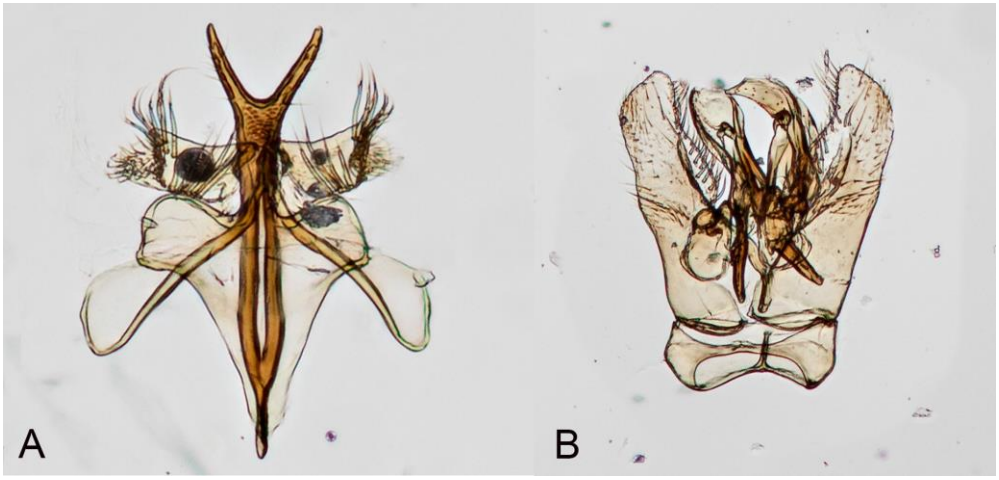


**Figure 7:** Terminalia of *C. paveli.* A, S7 and S8; B, Genital capsule.

***Chilicola* (*Hylaeosoma*) *liudmilae* Miklasevskaja**

**Holotype.** ♀, Bolivia, La Paz (23.III.2001 [23 March, 2001], Parker. Colletidae: *Chilicola* (*Hylaeosoma*) sp. N., Det. Miklasevskaja, 2016. Specimen is in excellent condition and is deposited in the Packer Collection at York University (PCYU) in Toronto, Ontario, Canada.

**Paratypes:** 16 females with the same locality and date information as the holotype.

**Diagnosis.** This species can be differentiated from all others except *C. aequatoriensis* and *C. paveli* by its wide head with length at most 1.05X its width, all other species have the head at least 1.15X as long as wide. Head of *C. paveli* males is wider than long, although might be more round in the unknown female, while in *C. aequatoriensis* length to width ratio is identical to *C. liudmilae.* It can be differentiated from *C. aequatoriensis* by its less densely punctate and sculptured head, with punctures separated at least 2X MOD on clypeus, paraocular area and vertex - surrounded by smooth and relatively shiny ground. Head of *C. aequatoriensis* females is coarsely and densely punctate, with microstriate clypeus. Mesoscutum punctation is unique to this species with its variable punctures, majority larger in diameter than the parapsidal line.

**Description.** ♀: *Structure*: Body length 5.38 mm; forewing length 3.2 mm, intertegular distance 0.83 mm. Head almost round (Fig. 6C), length 1.05 mm, width 1.00 mm; UOD 0.6 mm, LOD 0.39 mm; paraocular area slightly impressed for reception of scape, depression terminating below level of upper tangent of compound eye; pedicel as broad as and about half as long as scape; F1 half as long as pedicel and about as long as broad; F2-F5 broader than long; F6-F9 as long as broad; malar area linear; occeloccipital distance 1.2MOD as measured from margin of

the sharply rounded preoccipital ridge; T1 length and breadth subequal (0.62mm: 0.68mm respectively).

*Sculpturing*: Integument mostly dull and coarsely microsculptured (as in other species of the *longiceps* group); punctures on clypeus, paraocular area and vertex separated by at least 2X puncture diameter, separated by a smooth relatively shiny ground; mesoscutum with large punctures at least as large as the width of parapsidal line, on a roughened ground; scutellum with small punctures on shining ground both separated by at least one puncture diameter; impunctate, shiny fovea mesad of concavity of compound eye, marked by lateral carina; metapostnotum rugose anteriorly with irregular median carina.

*Coloration*: Integument predominantly black (Fig. 6C, D); head black except dark brown mandible and lighter brown F6-F10; tegula translucent, dark brown; forewing venation dark brown; hind wing venation light brown; wing membrane infumate; preepisternum, mesepisternum and metepisternum black; legs dark brown; metasoma dark brown.

*Pubescence*: Mostly white; head with scattered, minute largely simple setae, 0.5-1MOD in length, except on paraocular and frontal areas branched and longer, 1.5-2MOD in length. Mesoscutum and mesoscutelum with relatively short and sparse setae; pronotum with denser, simple, short setae; metanotum with relatively long setae, 1.5MOD, on lateral areas; meso- and metapleuron with sparsely scattered, medium length, branched setae; lateral surface of propodeum with branched medium setae all over, except minute and simple setae dorsally; ventral surface of coxae, protrochanter, profemur and metatibia with relatively long simple setae, 1MOD in length; anterior surface of pro- and mesofemora with minute, sparsely scattered setae; metafemur with long branched setae, 1.5MOD in length. Metasoma with relatively long setae

throughout, 1MOD in length, denser and longer on lateral apical margins of terga; sterna with visibly longer setae; S1 with eight long and plumose setae, 2-3MOD in length, S2 setation as in S1 but denser laterally; S3-S6 with long simple and branched setae, 1-2MOD in length.

**Etymology:** In memory of my mother, Liudmila Miklasevskaja, in recognition of the considerable sacrifices she has made for her children. It is formed in the genitive singular case.

***Chilicola* (*Hylaeosoma*) *boyacense* Miklasevskaja**

**Holotype.** ♀, Colombia, Boyaca (17.v-5.vi. 2001) [May 17-June 3, 2001], Reina Colletidae: *Chilicola* (*Hylaeosoma*) sp. N., Det. Miklasevskaja, 2015. Specimen is in an excellent condition and is currently deposited in PCYU. I

**Paratypes:** 16 more females from the same locality as the holotype. Three females 17.v-5.vi.2001. Two females 10-28.vi.2001. Two females 29.i-14.ii.2001. Two females 5-26.iii.2001. Two females 25.x-16.xi.2001. Three females 16.xi-1.xii.2001. One female 21.vi-6.vii.2001. One female 31.viii-16.ix.2001.

**Diagnosis.** Females of this species can be differentiated from other members of the subgenus, except *C. rugotergata* and *C. smithpardoi* by its densely punctate T1, with most punctures separated by a puncture diameter or less, the others have [most] punctures separated by more than a puncture diameter. It can be differentiated from *C. rufotergata* by its almost entirely pale mandibles, which are dark in *C. rufotergata,* and from *C. smithpardoi* by a stigmal perpendicular which is in the apical half of the second submarginal cell as opposed to being apical to the second recurrent vein in *C. smithpardoi*.

**Description.** ♀: *Structure*: Body length 5.1 mm; forewing length 3.2 mm, intertegular distance 0.77 mm. Head slightly elongate (Fig. 8A), length 1.05 mm, width (as measured from apex of clypeus to lower margin of median ocellus) 1.00 mm; UOD 0.7 mm, LOD 0.47 mm; paraocular area deeply impressed for reception of scape, depression terminating below the upper tangent of compound eye; pedicel as broad as and about half as long as scape; F1 slightly shorter than pedicel and 1.3× longer than broad; F2-F6 broader than long; malar area linear; occeloccipital distance 1MOD as measured from margin of the sharply rounded preoccipital ridge; T1 broader than long (0.95mm:0.68mm respectively).

*Sculpturing*: Integument mostly dull and coarsely microsculptured (as in other species of the *longiceps* group); mesoscutum, scutellum with punctures separated by one puncture diameter surrounded by micro-punctured ground; metapostnotum with parallel rugae and a distinct median carina; impunctate, shiny fovea mesad of concavity of compound eye with mesal pore 4 puncture diameters in length, marked by lateral carina; depression for reception of scape shiny with small punctures as dense as on frons; clypeus, supraclypeal area and mesepisternum with punctures separated by one or more puncture width surrounded by micropunctured ground; vertex with dense punctures nested in reticulate ground.

*Coloration*: Integument predominantly black (Fig. 8A, B); head black except yellow labiomaxillary complex, mandible and posterior of F5-F10; apex of mandibles amber red, base dark brown; tegula translucent, testaceous; forewing venation brown, pterostigma brown; hind wing venation light brown; wing membrane infumate; legs predominantly brown except apex of femora, extremities of tibia, basi- and miditarsi honey yellow; abdominal terga brown except

apical margins of T1-T6 translucent light-brown; sterna dark brown, except S2-S5 apical margin honey yellow medially.

*Pubescence*: Mostly white; head with minute simple setae, <0.5MOD in length, except longer, 1OD, on genal and hypostomal areas. Mesosomal setae minute, except more dense and branched around pronotal lobe; mesoscutum and mesoscutelum with minute setae, 0.5MOD in length; pronotum with dense, simple, short setae branching at posterior margin; metanotum with short branched setae, 0.5-1MOD, curved medially; meso- and metapleuron with sparsely scattered, minute, branched setae, getting progressively longer ventrally, reaching 1MOD in length; lateral surface of propodeum with simple minute setae all over, except longer and branched setae dorsally; coxae and trochanters with short hair. ventral surface of pro- and mesofemur with minute setae <0.5MOD in length; long branched setae on metafemur; protibia with longer curved and capitate hairs, mesotibia with short and branched setae, metatibia with short simple setae. Metasoma with minute setae throughout, except longer and branched on lateral apical margins of T1-T4 and progressively longer towards apex; sterna with visibly longer setae; S1 with ten long plumose setae, 4-5MOD in length; S2 and S3 with setae as S1 but denser; S4-S5 with long branched setae apically; S6 setae long and simple.

**Etymology:** A noun term for Boyaca, a city of origin.

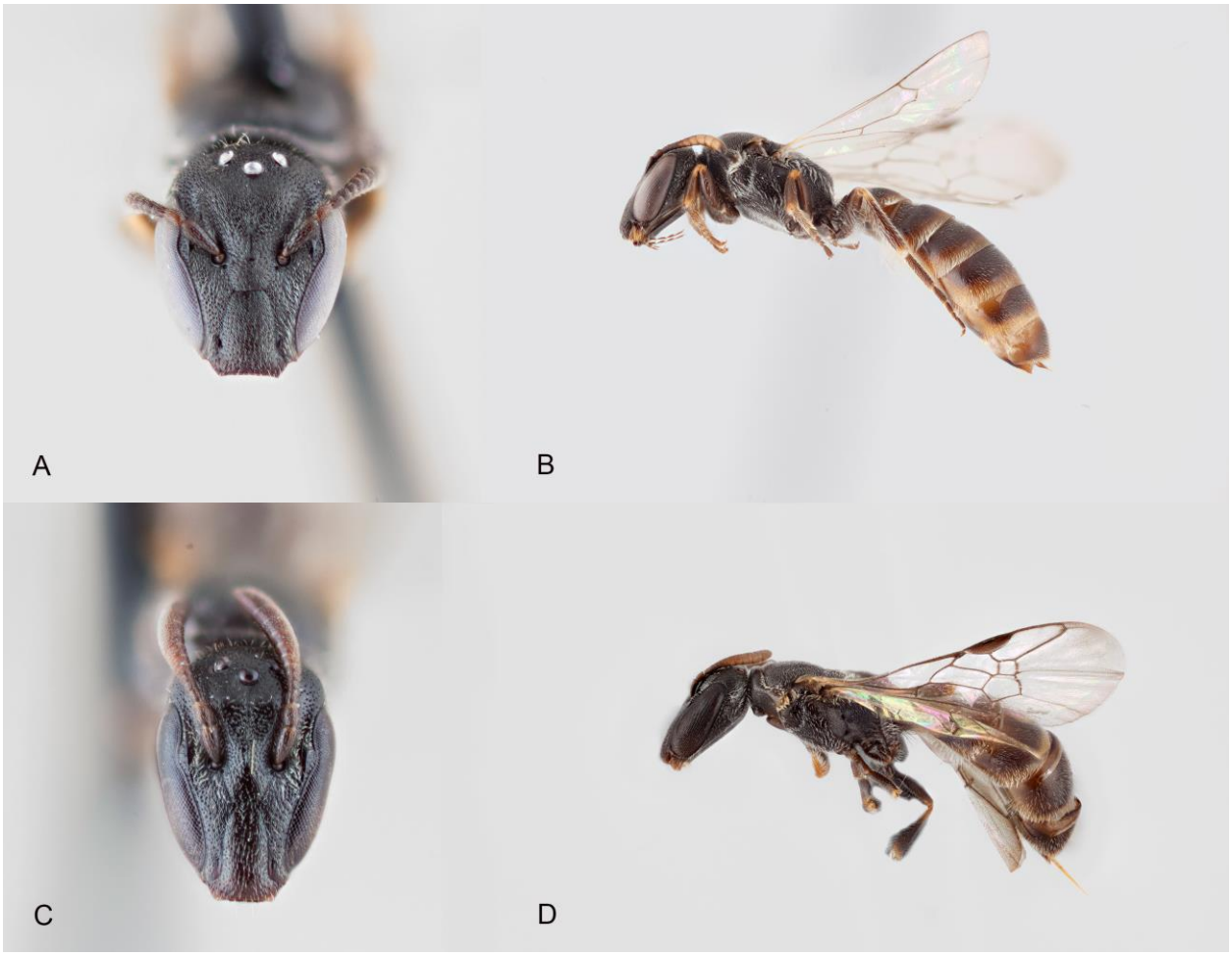


**Figure 8:** *Chilicola boyacense* (A, B) and *C. boliviana* (C, D).

***Chilicola* (*Hylaeosoma*) *boliviana* Miklasevskaja**

**Holotype.** ♀, Bolivia, Santa Cruz, N Boyuibe (5.III.1999) [March 5, 1999], Irwin/Parker, Colletidae: *Chilicola* (*Hylaeosoma*) sp. N., Det. Miklasevskaja, 2016. Specimen is missing all tarsi except one probasitarsus and is currently deposited in PCYU.

**Diagnosis.** Females of *C. boliviana* can be differentiated from all others in the subgenus by the pubescence of the lateral surface of propodeum, which is uniformly short and sparse throughout. All other species have variable hair length above and below, with the exception of *C.*

*yanezae* and *C. rufotergata.* Unlike the shiny and sparsely punctate (separated by 2X puncture width or more) integument of *C. yanezae, C. boliviana* females possess a dull and more densely punctate integument (punctures separated by 2X puncture width or less). S2 hairs of *C. boliviana* females are plumose as opposed to with only few long branches on the anterior of rachis, found in *C. rufotergata* females.

**Description.** ♀: *Structure*: Body length 4.8 mm; forewing length 3.2 mm, intertegular distance 0.69 mm. Head elongate (Fig. 8C), length 1.02 mm (as measured from apex of clypeus to lower margin of median ocellus), width 0.89 mm; UOD 0.57 mm, LOD 0.35 mm; paraocular area deeply impressed for reception of scape, depression terminating just above the upper tangent of compound eye; pedicel as broad as and about half as long as scape; F1 slightly shorter than pedicel and 1.2× longer than broad; F2 as broad as long; F3-F7 broader than long; malar area linear; occeloccipital distance 1.2MOD as measured from margin of the sharply rounded preoccipital ridge; T1 longer than broad (0.70mm:0.62mm respectively).

*Sculpturing*: Integument mostly dull and coarsely microsculptured (as in other species of the *longiceps* group); mesoscutum with punctures separated by one puncture diameter or more surrounded by tessellate shining ground; scutellum with punctures separated by one puncture diameter of less surrounded by smooth ground; metapostnotum rugulose; tergal punctures small and shallow, separated by at least 2X puncture diameter; impunctate, shiny fovea mesad of concavity of compound eye, marked by lateral carina; depression for reception of scape shiny with small punctures separated by 2 punctures width; clypeus and supraclypeal area with small punctures separated by one or more puncture width surrounded by somewhat smooth ground; frons and vertex with larger punctures nested in reticulate ground and separated by less that

puncture width diameter, except much sparser near ocellar area; genal area with variable punctures.

*Coloration*: Integument predominantly black (Fig. 8C, D); head black except brown labrum, mandible and labiomaxillary complex. Antennae brown except light brown posterior of F5-F9; tegula translucent, testaceous; forewing venation brown, pterostigma brown; hind wing venation light brown; wing membrane infumate; legs predominantly brown except apex of femora, extremities of tibia, probasitarsus honey yellow; abdominal terga brown except apical margins of T1-T6 translucent light-brown; sterna brown, except S3 and S4 apical margin honey yellow medially.

*Pubescence*: Mostly white; head with minute simple setae, <0.5MOD in length, except on paraocular and hypostomal ares denser and branched. Mesosomal setae minute, except more dense and branched around posterioir margin of pronotal collar and pronotal lobe; mesoscutum and mesoscutelum with minute setae, 0.5MOD in length; pronotum with dense, simple, short setae; metanotum with short branched setae, 0.5-1MOD, curved medially; mesopleuron with short, branched setae, 0.5-1MOD in length; metapleuron and lateral surface of propodeum with simple minute setae all over, branching dorsally; procoxa, protrochanter, pro- and mesofemora with sparsely scattered, simple minute setae; meso- and metacoxae, mesotrochanter and tibia with simple short hairs; ventral surface of probasitarsus with short capitate setae; metatrochanter and metafemur with relatively long, 1.5-2MOD in length, branched setae. Metasoma with minute setae throughout; sterna with visibly longer setae; S1 with 8-10 long plumose setae, 3-4MOD in length; S2 and S3 with setae as S1 but denser; S4-S5 with long sparse setae apically; S6 setae denser than in preceding sterna.

**Etymology:** An adjectival form based on Bolivia, country of origin.

***Chilicola* (*Hylaeosoma*) *lambayequense* Miklasevskaja**

**Holotype.** ♀, Peru, Lambayeque (21.V.1996) [May 21, 1996], Rozen/Ugarte, Colletidae: *Chilicola* (*Hylaeosoma*) sp. N., Det. Miklasevskaja, 2016. Specimen is missing both hind legs and left flagellum and is currently deposited in PCYU.

**Diagnosis.** Females of *C. lambayequense* possess a unique stigma and pubescence on S2, not found in any other species of the subgenus. In *C. lambayequense,* the stigmal margin in the marginal cell is angularly convex, as opposed to smoothly convex in all other species. The hairs on S2 have numerous short anterior branches, unlike the plumose hairs or hairs with a few long anterior branches in other species of the subgenus.

**Description.** ♀: *Structure*: Body length 5.4 mm; forewing length 3.4 mm, intertegular distance 0.74 mm. Head elongate (Fig. 9A), length 1.15 mm (as measured from apex of clypeus to lower margin of median ocellus), width 1.00 mm; UOD 0.64 mm, LOD 0.46 mm; paraocular area deeply impressed for reception of scape, depression terminating 0.5MOD below the upper tangent of compound eye; pedicel as broad as and about half as long as scape; F1 slightly shorter than pedicel and 1.5× longer than broad; F2 and F3 as broad as long; F4-F7 broader than long; malar area linear; occeloccipital distance 1.2MOD as measured from margin of the sharply rounded preoccipital ridge; T1 shorter than broad (0.75mm:0.95mm respectively).

*Sculpturing*: Integument mostly dull and coarsely microsculptured (as in other species of the *longiceps* group); mesoscutum and scutellum with punctures separated by one puncture diameter or less surrounded by micropunctured shining ground; metapostnotum rugulose with a

distinct median carina; impunctate, shiny fovea mesad of concavity of compound eye, marked by lateral carina; depression for reception of scape shiny with small punctures less dense that elsewhere on the head; clypeus and supraclypeal area with small punctures separated by approximately one puncture width surrounded by roughened ground; frons and vertex with similar sized punctures nested in lightly rugose ground; genal area with punctures as on vertex, separated by one or more puncture diameter on a smooth ground.

*Coloration*: Integument predominantly black (Fig. 9); head black except brown labiomaxillary complex and honey brown spot on mandibles. Antennae brown except light brown posterior of F5-F10; tegula translucent, testaceous; forewing venation brown, pterostigma brown; hind wing venation light brown; wing membrane infumate; legs predominantly brown except apex of femora, extremities of tibia, tarsi light brown; abdominal terga brown except apical margins of T1-T6 translucent light-brown; sterna brown, except S1-S4 apical margin light brown.

*Pubescence*: Mostly white; head with minute simple setae, <0.5MOD in length, except longer on labrum, vertex and hypostomal (~1MOD). Mesosomal setae minute, except more dense and branched around posterioir margin of pronotal collar and pronotal lobe; pronotum, mesoscutum and mesoscutelum with minute setae, <0.5MOD in length; metanotum with short branched setae, 0.5-1MOD, curved medially; mesopleuron with minute, branched setae above and short, branched setae, 0.5-1MOD in length below; metapleuron and lateral surface of propodeum with simple minute setae all over, branching dorsally; pro- and mesocoxae with short simple setae, metacoxa with longer (~1MOD), branched setae; protrochanter, pro- and mesofemora with simple minute setae; mesotrochanter and tibia with simple short hairs; ventral surface of probasitarsus with short (1MOD) apically bent setae. Metasoma with minute setae

throughout; sterna with visibly longer setae; S1 with twelve long plumose setae, 3-4MOD in length; S2 and S3 with setae as S1 but denser laterally; S4-S5 with simple, long sparse setae apically; S6 setae denser than in preceding sterna.

**Etymolgoy:** A noun term for Lambayeque, a city of origin.

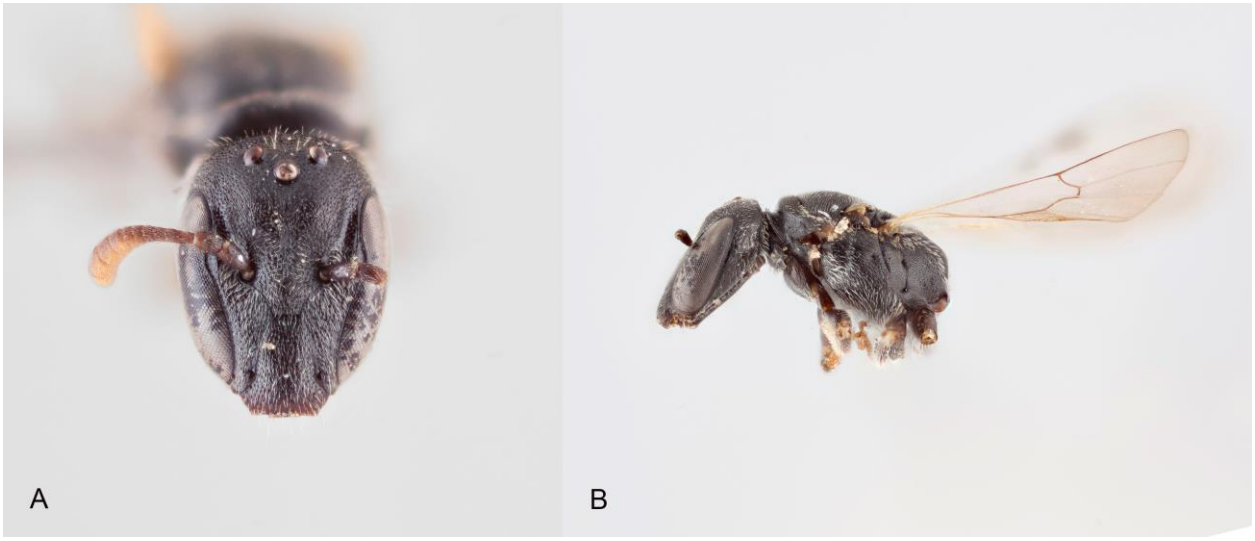


**Figure 9:** *Chilicola lambayequense.*

*Geometric Morphometrics*

PLS test for independence between characters showed varying results for different pairwise combinations analyzed. For individual specimens as well as with individuals within species pooled, combinations with higher *RV* scores, with the lowest being 0.5718 and highest 0.6051, (Table 2) were strongly supported in the permutations tests, while those with low *RV* values (*RV*=0.0774, 0.123, 0.1318) had non-significant associations. When the categorical factor of species is corrected for in a pooled within species analysis the *RV* value decreases for most comparisons (Table 2). Considering statistically significant results only, overall, there seems to be very low correlation between configurations (RV ranging from 0.2531 to 0.3298).

MANOVA results revealed significant ($P$<0.05) differences among species for all configurations (Table 3). Wilk's Lambda value was almost zero in all axes of C1-C3 implying that most of the variance is explained by the independent variable. Although, Wilk's Lambda in C4 is higher,most shape change is still attributed to the independent variable. Combination of low p-values and low Wilk's Lambda confirms that *a priori* established groups are indeed different.

**Table 2:** RV coefficients and P-values from the corresponding PLS analysis for different configurations of *C. (Hylaeosoma)* wing venation.

| | Individual specimens | | Pooled within species | |
|---|---|---|---|---|
| Comparison | *RV* | *P*-value | *RV* | *P*-value |
| C1 vs. C2 | 0.5718 | <0.0001 | 0.2201 | 0.057 |
| C1 vs. C3 | 0.5926 | <0.0001 | 0.3298 | 0.0088 |
| C1 vs. C4 | 0.0774 | 0.3012 | 0.084 | 0.3198 |
| C2 vs. C3 | 0.6051 | <0.0001 | 0.3172 | 0.0022 |
| C2 vs. C4 | 0.123 | 0.1172 | 0.2531 | 0.0062 |
| C3 vs. C4 | 0.1318 | 0.125 | 0.1306 | 0.1426 |

**Table 3:** Values obtained in the CVA, including MANOVA test of significance conducted in CVAGen.

| Configuration | Axis | Wilk's Lambda | $X^2$ | *d.f.* | *P*-value |
|---|---|---|---|---|---|
| 1 | 1 | 0.00001 | 266.8305 | 120 | <0.0001 |
| | 2 | 0.00001 | 187.217 | 99 | <0.0001 |
| | 3 | 0.00001 | 138.2029 | 80 | <0.0001 |
| | 4 | 0.0001 | 95.0911 | 63 | 0.0056 |
| 2 | 1 | 0.00001 | 401.0405 | 176 | <0.0001 |
| | 2 | 0.00001 | 293.5384 | 150 | <0.0001 |
| | 3 | 0.00001 | 227.7113 | 126 | <0.0001 |
| | 4 | 0.00001 | 173.7733 | 104 | <0.0001 |
| | 5 | 0.0004 | 124.5054 | 84 | <0.0001 |
| 3 | 1 | 0.00001 | 401.747 | 224 | <0.0001 |
| | 2 | 0.00001 | 314.0674 | 195 | <0.0001 |
| | 3 | 0.00001 | 236.1277 | 168 | 0.0004 |
| | 4 | 0.00001 | 186.3262 | 143 | 0.0087 |
| 4 | 1 | 0.0529 | 55.8516 | 30 | 0.0028 |
| | 2 | 0.2694 | 24.9177 | 14 | 0.0354 |

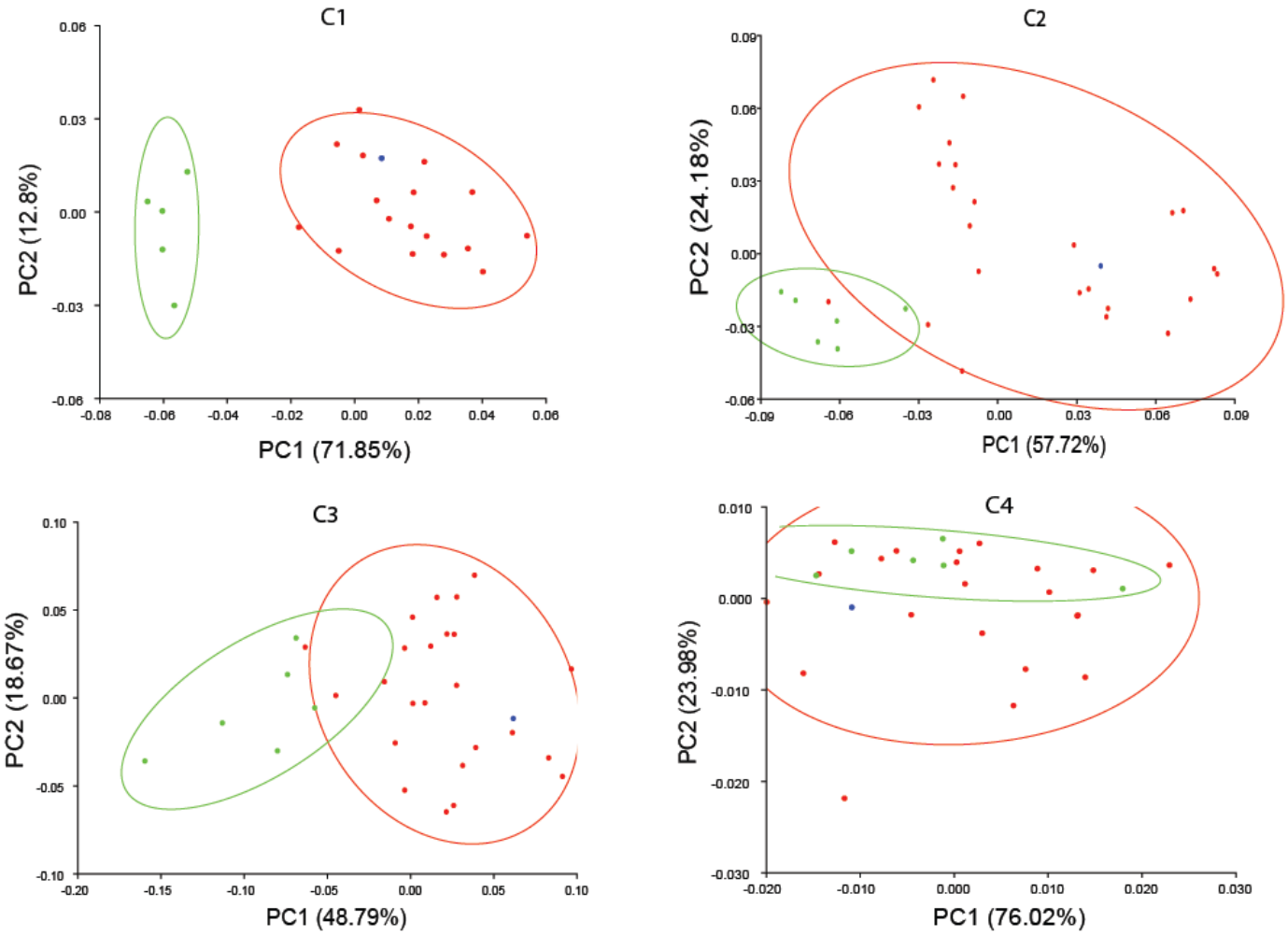


**Figure 10:** Confidence ellipses (95%) showing morphogroup separation in each of the four configurations, C1-C4, generated in MorphoJ. Each mark represents a specimen. *Megalostigma* group is represented in green, *longiceps* group is red, the outgroup is blue. Axes x and y represent axes 1 and 2 from table 3, respectively.

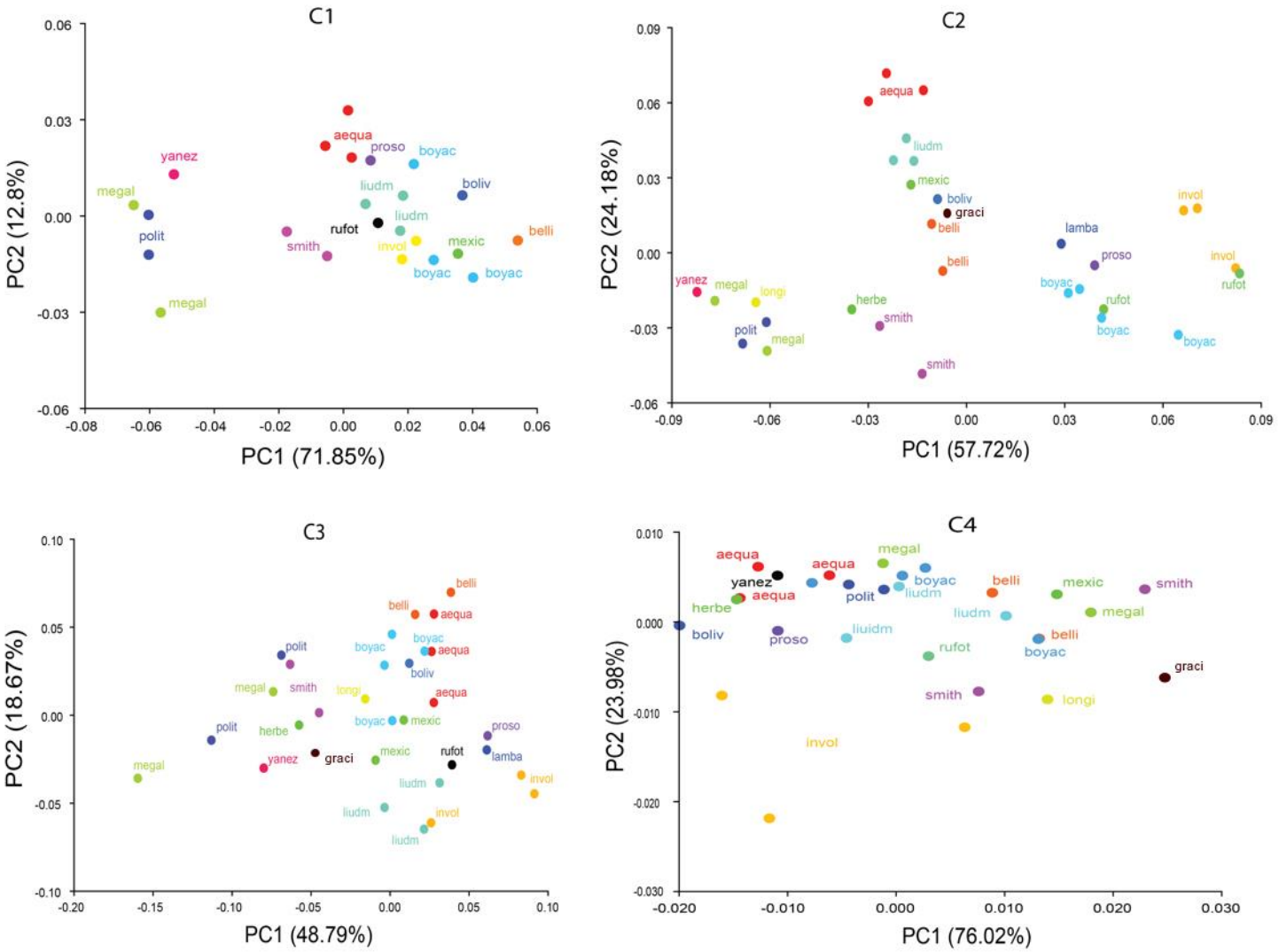


**Figure 11:** PCA scatter plot of specimens grouped into species by colour.

PCA of C1 showed considerable dispersion across morphospace between morphogroups. The first principal component explained 71.85% of the total variance – describing changes mostly in the lengthening of the radial cell in the direction of basal to distal in the *longiceps* group. No clear separation on other axes between morphogroups or among species within morphogroups is observed (Figs. 10, 11).

PCA of C2 shows less separation of two morphogroups than in C1, with PC1 explaining 57.72% of the variance reflecting expansion of the stigma and shortening of the anterior margin of the second submarginal cell in the *megalostigma* compared to the *longiceps* group. Some

species separation is noted on PC2 (24.18% of variance explained), clearly separating *C. aequatorienses* and *C. liudmilae* both from each other and from the rest. Those specimens possess a more elongate stigma as well as a longer anterior margin of the second submarginal cell (Figs. 10, 11).

PCA of C3 also shows separation of the two morphogroups along PC1 (48.79%) although with some overlap. PC1 describes a lengthening at the posterior and minor narrowing at the distal ends of the second medial cell. PC2 offers no separation, however the *longiceps* group occupies a considerably larger morphospace than the *megalostigma* group, displaying variance in the length of the posterior margin of the second submarginal cell within the group (Figs. 10, 11).

Individual PC's of C4 PCA (PC1=76.02%, PC2=23.98%) showed no clear separation of groups and only a weak separation of *C. involuta* from the rest, occupying a more negative morphospace on both axes reflected by a smaller distance between landmarks 2 and 3 (Figs. 10, 11).

**Table 4:** Results of Jackknife grouping test in CVAGen. Actual values represent percentage of specimens assigned to the correct group, whereas random values represent the percentage expected with a random rate of correct assignments.

| | Species | | Morphogroup | |
|---|---|---|---|---|
| | Actual | Random | Actual | Random |
| C1 | 88.24 | 16.96 | 100 | 65.97 |
| C2 | 69.57 | 12.29 | 93.55 | 68.78 |
| C3 | 34.78 | 14.18 | 90.32 | 65.04 |
| C4 | 14.29 | 15.65 | 62.07 | 50.54 |

CVA Jackknife analysis confirmed significant taxonomic signal in C1, C2 and C3: 100%, 93.55% and 90.32%, respectively, of all the individuals were assigned to the correct morphogroups. C4 had a 62.07% of correct assignments, as opposed to 50.54% expected at random for the morphogroup, and thus showed no important taxonomic value. C1 and C2

showed a significant taxonomic signal for placement of specimens into their assigned species (Table 4), whereas only 34.78% of specimens were placed into their right species based on the shape of C3 and only 14.29% based on the shape of C4.

After mapping PC scores onto the morphological phylogeny, a permutation test for phylogenetic signal revealed significant signal for C1, C2 and C3 (*P*=0.0077, *P*=0.0035 and *P*=0.0031, respectively). No phylogenetic signal was observed in C4 (*P*=0.7453). In addition, C4 displays a high level of homoplasy, as illustrated in Figure 12 by a large number of reversals between morphogroups.

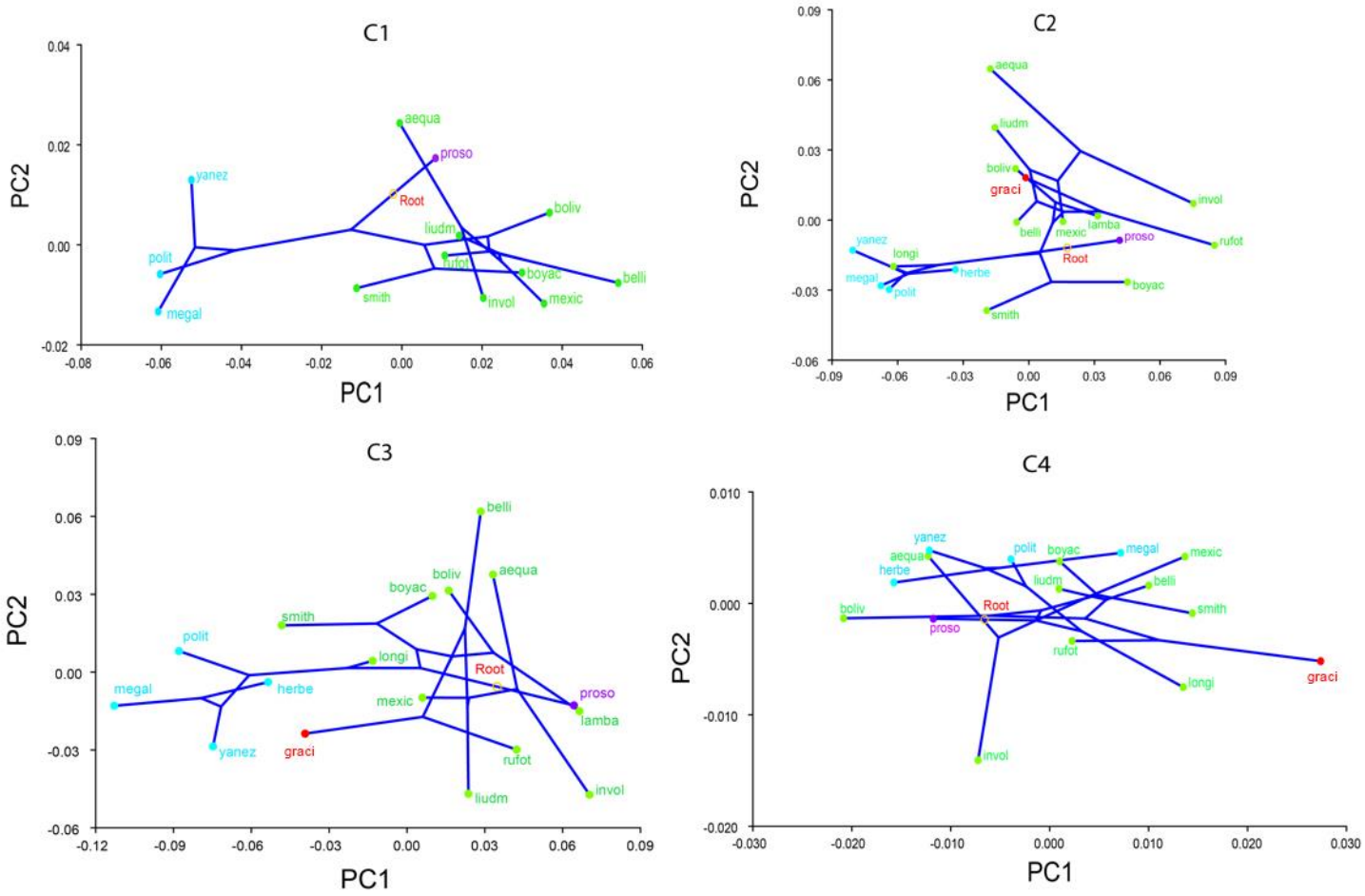


**Figure 12:** Wing shape PC scores mapped onto a phylogeny to test for phylogenetic signal and view homoplasy. Blue, green, red and purple colours represent *megalostigma*, *longiceps*, fossil and outgroup, respectively.

*Phylogenetic Results*

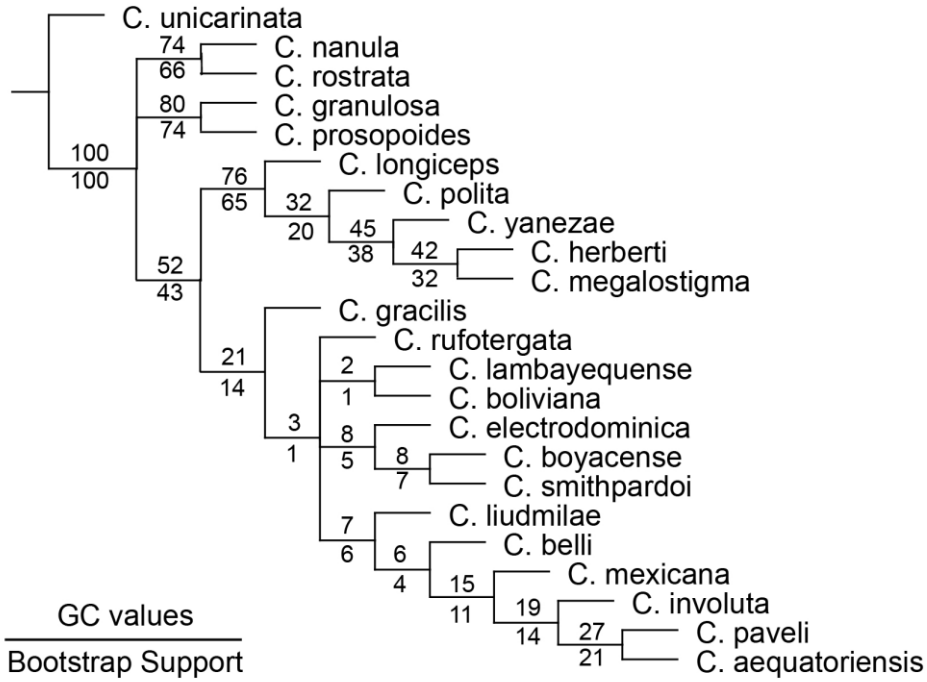


A

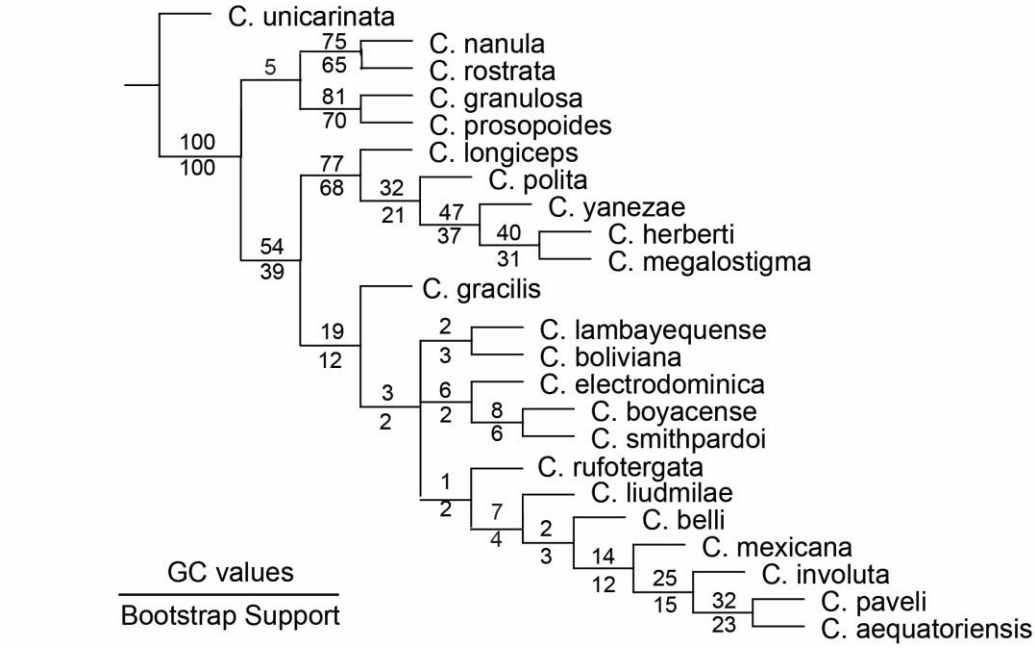


B

**Figure 13:** Results of unweighted maximum parsimony analyses. Support values were calculated based on 500 permutations, GC values are indicated above the branch, bootstrap support – below. A: discrete morphological characters only, B: discrete morphology combined with geometric morphometrics.

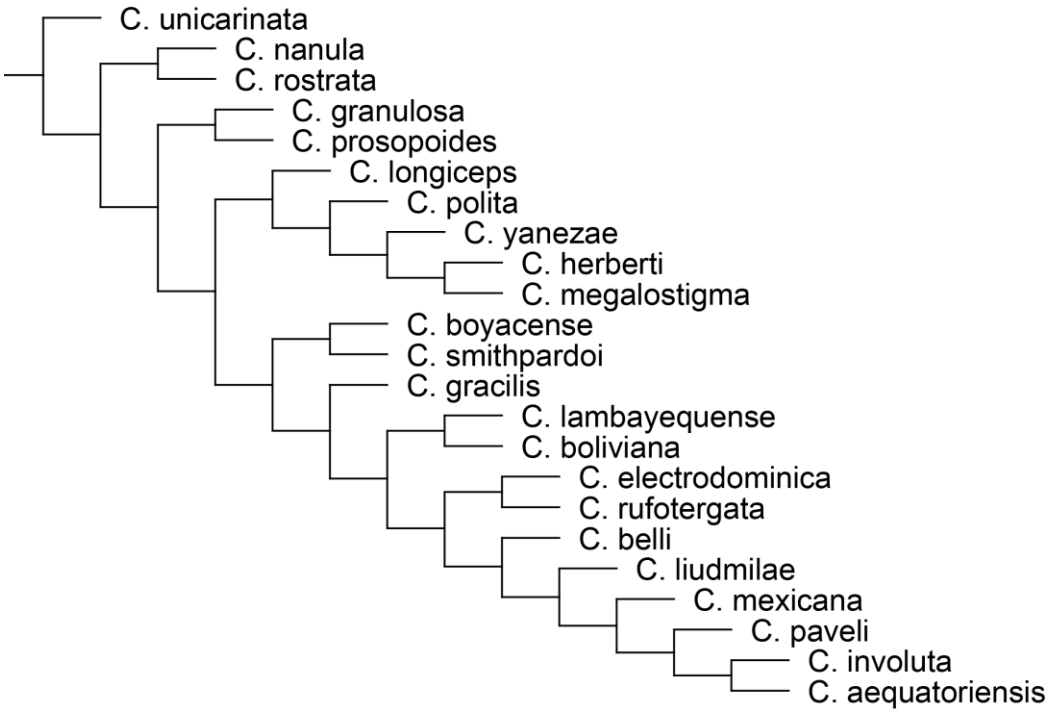


**Figure 14:** Result of the weighted analyses under implied weights. Identical tree obtained for discrete morphology alone and combined datasets.

Ninety-two discrete morphological and three shape characters were included in the phylogenetic analysis. The fourth wing configuration was excluded from analyses due to non-significant phylogenetic signal as noted above. The phylogenetic analysis of discrete morphology alone produced 17 most parsimonious trees with 406 steps, consistency index (CI) of 0.426 and retention index (RI) of 0.538. As a result, some groups were found to be unresolved in the consensus tree (Figure 13A). Analysis of discrete morphological characters combined with geometric morphometrics produced a single most parsimonious tree with 414.99 steps, CI of 0.414 and RI of 0.504 (Figure 13B), resolving the outgroup node as well as improving the resolution of the node that contains all of the *longiceps* group species except for *C. longiceps* and *C. gracilis*. Addition of three shape configurations resulted in a slight increase in support for the following groups: all the *megalostigma* group, except for the *C. herberti + C. megalostigma*

species pair; as well as *C. paveli + C. aequatoriensis* and [*C. paveli + C. aequatoriensis*] + *C. involuta* nodes.

Monophyly of *C.* (*Hylaeosoma*) is rather well supported and it is defined by stigma perpendicular extending beyond the apical half of the second submarginal cell, comma shaped anterior tentorial pit (except in *C. smithpardoi* and *C. boyacense* in which the anterior tentorial pit is oval in shape) and dark paraocular areas in males. *Chilicola* (*Hylaeosoma*) contains two clades. One is the relatively well supported *megalostigma* morphogroup with *C. longiceps* of the *longiceps* group sister to the rest of this group. The group is defined by a short scape and flat or concave margin between vertex and occiput. However, in *C. megalostigma* and *C. herberti* the scape reverts to normal length. The other clade is a weakly supported *longiceps* morphogroup without *C. longiceps,* defined by a bifurcate S8 apical process that is either broad or crescentic as opposed to the longer and more narrow processes of the *megalostigma* group plus *C. longiceps*. I propose the *aequatoriensis* species group as an alternative name for this clade, named after the first discovered species of that clade.

Implied weighting produced identical trees for both morphological and combined datasets (Figure 14). The weighted analysis tree differs from the unweighted tree by having *C. boyacense* and *C. smithpardoi* sister to all other members of the *aequatoriensis* group, *C. rufotergata* sister to *C. electrodominica, C. belli* diverging prior to *C. liudmilae,* and *C. involuta* as sister to *C. aequatoriensis* (Fig. 14). In both trees *C. longiceps* was placed as the earliest diverging species of the *megalostigma* morphogroup, rendering the *longiceps* morphogroup paraphyletic.

Fossil placement is rather consistent among trees - *C. gracilis* shows an earlier divergence than *C. electrodominica,* being the earliest diverging species of the *aequatoriensis* group in the unweighted tree and sister to (*C. smithpardoi + C. boyacense)* with the three species forming a

clade sister to the remaining species of the *aequatoriensis* group in the weighted tree. Both fossils. albeit from the Dominican Republic, are grouped with species found in Peru and Bolivia only, they do not group with the extant Caribbean species.

## Discussion

The study here presents a first phylogenetic analysis incorporating the morphology of Colletidae fossils. Previous studies have used these fossils in a node-dating approach (Almeida et al. 2011, Cardinal and Danforth 2013, Kayaalp et al. 2017), whereas, here the evolutionary relationship of the fossils and extant species is established for the first time. To maximize the amount of signal extracted from fossils, geometric morphometric analyses were performed on forewings landmarks and included in the phylogenetic analysis.

Addition of geometric morphometrics data for the LAUP proved to be a useful addition evidenced by stronger support and increased resolution of polytomies for some groups.

Incorporation of geometric morphometrics into phylogenetic analysis is a rather recent and a controversial practice. A multitude of studies have employed this method with varying levels of success.

For example, Ferdous (2013, unpublished dissertation) used shape and qualitative morphology to construct a phylogeny of *Mystus* sp. (Chordata, Bagridae) and concluded that while geometric morphometrics possess a strong phylogenetic signal and can complement a qualitative dataset, shape data alone is not sufficient to produce a robust phylogeny. The study also noted that geometric morphometrics are important in analyzing character shape evolution from existing phylogenies.

De Meulemeester et al. (2012) and Michez et al. (2009) are the only two studies so far that have attempted to use geometric morphometrics to construct a relationship tree for bees. The former employed clustering methods to generate a phenetic relationship, whereas the latter used a matrix of similarities based on Euclidian distances to construct a Neighbour-joining tree. Neither of the studies performed a maximum parsimony analysis to infer phylogenetic relationships from shape data.

Perrard et al. (2016) conducted the first study employing LAUP for Vespinae wasps and, in addition to conventional analyses, ran simulations to test for accuracy and effectiveness of landmark data. Their results suggested that methods available at the time of study implementing landmarks might overestimate resolution of nodes, and stressed the importance of resampling in TNT to collapse those nodes that were weakly supported. In addition, they found that wing venation is not a very reliable character when used alone for that group, however, they did find that it can provide useful insight into unresolved clades. As opposed to Perrard et al. (2016) this study uses newly developed methods for landmark analyses under parsimony made available by the new version of TNT (Goloboff and Catalano 2016). This new methodology serves to solve the issue of overestimated resolution . In contrast to Perrard et al. (2016), wing venation in this study has been, for the most part, useful, with strong phylogenetic signal for 3 of the 4 configurations. However, analyses of the shape data herein suggest that more intricate forewing configurations are more useful in phylogenetic analyses as well as for differentiating between morphogroups as opposed to shapes with fewer landmark points. C4, containing only three landmarks, does not possess a significant phylogenetic signal nor is it useful in assigning specimens into species or morphogroups. It is possible that C4 is not an informative character due to insufficient shape information integrated into that confirmation by only three landmarks.

It seems that a balance needs to be found between the number of configurations used in the LAUP and the number of landmarks in each configuration, since Catalano and Torres (2017) recommend the use of more than one configuration in LAUP, and Roth (1993) as well as the results of shape analyses presented herein reveal that the use of more landmarks in order to encompass more structural variation can be more useful. Therefore, when a structure is broken up into configurations, it might be helpful to favour fewer configurations containing more landmarks in each.

Overall forewing venation patterns were significantly different between the *longiceps* and the *megalostigma* morphogroups. Species of the *megalostigma* morphogroup possess a seemingly more swollen stigma and a smaller second submarginal cell with respect to the rest of the structure compared to the species of the *aequatoriensis* group, while in *C. longiceps* of the *longiceps* group the stigma is also more swollen and pronounced occupying an intermediate position in the phylogeny. Danforth et al. (1989) discusses adaptive variation in the hymenopteran stigma and notes that stigma size tends to be larger in proportion to the rest of the wing in smaller individuals. In this case, however, notably larger bees of the *megalostigma* group possess a larger stigma. Danforth et al. (1989) mentioned that the stigma potentially serves as a means of shifting a centre of mass of the animal in flight and enhancing changes of wing shape in flight, however, but did not provide any insight into flight patterns associated with various stigma sizes.

Geographic distribution of the *megalostigma* and *aequatoriensis* clades reveal interesting patterns. Members of the *megalostigma* group tend to inhabit low elevation areas ranging from 270-1944m, whereas those of the *aequatoriensis* group occupy higher altitudes, ranging from (1125-3694m). *Chilicola longiceps* shares characteristics of the *megalostigma* group by

inhabiting areas as low as sea level and up to 1822m. In addition, with the exception of one record of *C. megalostigma,* semi-arid and dry sub-humid habitats are inhabited predominantly by *longiceps,* while humid areas are inhabited by both clades (Figure 15).

Michener's (1992) suggestion that the *longiceps* group might be paraphyletic is strongly supported by the phylogenetic results: the highest node support within *C. (Hylaeosoma)* places *C. longiceps* within the *megalostigma* group.

The fossil placement in both weighted and unweighted trees suggests that *C. (Hylaeosoma)* is likely much older than the fossils' estimated age of 10-15 million year (Michener and Poinar 1996, Engel 1999). *Chilicola longiceps, C. boliviana* and *C. lambayequense* are all earlier diverging species than at least one of the fossils, while implied weight analysis suggests that *C. boyacense* and *C. smithpardoi* are also earlier diverging than either of the fossil species, suggesting that these extant lineages have survived for more than 10-15 million years.

Previous studies have incorporated *Chilicola (Hylaeosoma) spp.* fossils in order to calibrate Colletidae phylogeny. Almeida et al. (2011) used a Bayesian framework with assigned lognormal or normal *a priori* age to three nodes within Colletidae, one of which was Xeromelissinae, based on *Chilicola (Hylaeosoma)* spp. fossils. The resulting node ages for Colletidae, Xeromelissinae and *Chilicola* were 71 Ma, 42 Ma and 26 Ma, respectively. Cardinal and Danforth (2013) estimated divergence times for all the major groups of bees, employing a Bayesian framework with an uncorrelated relaxed-clock model, which allows for the rate of evolution among tree branches to vary, with probability of the ages applied to 15 nodes. Their results suggested a somewhat later age for Colletidae (68 Ma) and a notably later age for Xeromelissinae (25 Ma). Kayaalp et al. (2017) have used a 68 Ma node from Almeida et al. (2011) for Euryglossinae and Scrapterinae (two subfamilies of Colletidae otherwise not treated

herein) and have estimated a rather recent diversification of Xeromelissinae (17 Ma). Based on the findings of this study, it is probable that Kayaalp et al. (2017) underestimated the age of the Xeromelissinae, as demonstrated by *Chilicola gracilis* and *Chilicola electrodominica* being nested quite deeply among extant species of the subgenus. It is likely that *Chilicola* originated around 26 Ma, as stated by Almeida et al. (2011), giving Xeromelissinae a much older estimate of 42 Ma.

With information gained in this study, a more confident date estimate can now be placed on the *Chilicola* node, from which other nodes of the Colletidae can be calibrated. Combining this information with molecular data from *C. (Hylaeosoma)* will enable more precise Bayesian analyses for estimating divergence times and node ages.

Overall, geometric morphometric can be a beneficial tool when examining specimens with limited morphological information, such as in the study herein. LAUP has enabled placement of fossils into the phylogeny along with other extant taxa, and as a result provided insight into *C. (Hylaeosoma)* evolution.

**Table 5:** Elevation and climate ranges for known *Chilicola (Hylaeosoma)* localities. In some cases, labels contained elevation or latitude/longitude information only.

| Taxon | Habitat humidity | Elevation range (m) |
|---|---|---|
| *Chilicola longiceps* | hyper-arid, humid | 4-1822 |
| *Chilicola polita* | humid | 900-1942 |
| *Chilicola yanezae* | humid | 1000-1944 |
| *Chilicola herberti* | humid | -- |
| *Chilicola megalostigma* | semi-arid, humid | 270-900 |
| *Chilicola boliviana* | humid | 1500 |
| *Chilicola smithpardoi* | humid | 1125 |
| *Chilicola rufotergata* | hyper-arid | 3299 |
| *Chilicola liudmilae* | dry sub-humid | 2019 |
| *Chilicola belli* | semi-arid, humid | 1400-2120 |
| *Chilicola mexicana* | humid | 1130-3694 |
| *Chilicola involuta* | semi-arid | 3150-3200 |
| *Chilicola paveli* | humid | 2300 |
| *Chilicola aequatoriensis* | humid | 1900-2930 |

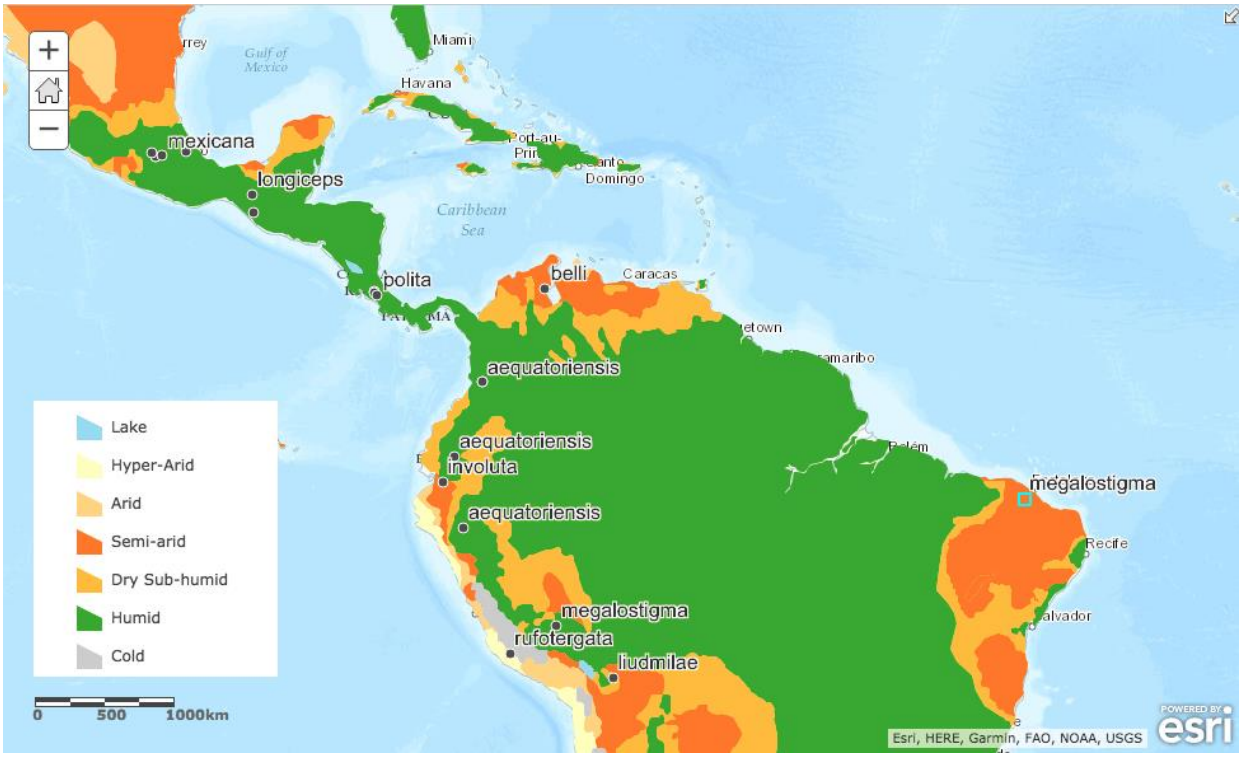


**Figure 15:** The map demonstrates the climatic divisions used in Table 5. The World Atlas of Desertification was published by UNEP in 1992 as the result of a cooperative effort between UNEP's Desertification Control Programme Activity Centre (DC/PAC), the Global Environment Monitoring System (GEMS) and the Global Resource Information Database (GRID).

## REFERENCES


Alexander, B. A., & Michener, C. D. (1995). Phylogenetic studies of the families of short-tongued bees (Hymenoptera: Apoidea). *The Univ. of Kansas science bull*, *55*(11), 377–424.

Almeida, E. A., Pie, M. R., Brady, S. G., & Danforth, B. N. (2011). Biogeography and diversification of colletid bees (Hymenoptera: Colletidae): emerging patterns from the southern end of the world. *Journal of biogeography*, *39*(3), 526-544.

Arcila, D., Pyron, R. A., Tyler, J. C., Ortí, G., & Betancur-R, R. (2015). An evaluation of fossil tip-dating versus node-age calibrations in tetraodontiform fishes (Teleostei: Percomorphaceae). *Molecular Phylogenetics and Evolution*, *82*, 131-145.

Ascher, J.S., and Pickering, J. 2016. Discover Life bee species guide and world checklist (Hymenoptera: Apoidea: Anthophila). Available from http://www.discoverlife.org/mp/20q?guide=Apoidea_species.

Bai, M., Beutel, R. G., Shih, C. K., Ren, D., & Yang, X. K. (2013). Septiventeridae, a new and ancestral fossil family of Scarabaeoidea (Insecta: Coleoptera) from the Late Jurassic to Early Cretaceous Yixian Formation. *Journal of Systematic Palaeontology*, *11*(3), 359-374.

Benoist, R. (1942). Les Hyménoptères qui habitent les tiges de ronce aux environs de Quito (Equateur). In *Annales de la Société Entomologique de France*, 111, 75-90.

Bookstein, F. L. (1994). The morphometric synthesis: a brief intellectual history. *Frontiers in Mathematical Biology*, 100, 212-237.

Brady, S. G., Litman, J. R., & Danforth, B. N. (2011). Rooting phylogenies using gene duplications: an empirical example from the bees (Apoidea). *Molecular phylogenetics and evolution*, *60*(3), 295-304.

Branstetter, M. G., Danforth, B. N., Pitts, J. P., Faircloth, B. C., Ward, P. S., Buffington, M. L., ... & Brady, S. G. (2016). Phylogenomic analysis of ants, bees and stinging wasps: improved taxon sampling enhances understanding of hymenopteran evolution. *Nature*, *27*, 1019-1025.

Brothers, D. J. (1976). Modifications of the metapostnotum and origin of the 'propodeal triangle in Hymenoptera Aculeata. *Systematic Entomology*, *1*(3), 177-182.

Brothers, D. J. (1999). Phylogeny and evolution of wasps, ants and bees (Hymenoptera, Chrysidoidea, Vespoidea and Apoidea). *Zoologica Scripta*, *28*(1-2), 233-250.

Cardinal, S., & Danforth, B. N. (2013). Bees diversified in the age of eudicots. *Proceedings of the Royal Society of London B: Biological Sciences*, *280*(1755), 20122686.

Cardinal, S., & Packer, L. (2007). Phylogenetic analysis of the corbiculate Apinae based on morphology of the sting apparatus (Hymenoptera: Apidae). *Cladistics*, *23*(2), 99-118.

Catalano, S. A., & Torres, A. (2017). Phylogenetic inference based on landmark data in 41 empirical data sets. *Zoologica Scripta*, *46*(1), 1-11.

Catalano, S. A., Goloboff, P. A., & Giannini, N. P. (2010). Phylogenetic morphometrics (I): the use of landmark data in a phylogenetic framework. *Cladistics*, *26*(5), 539-549.

Danforth, B. N. (1989). The evolution of hymenopteran wings: the importance of size. *Journal of Zoology*, *218*(2), 247-276.

Danforth, B. N., Eardley, C., Packer, L., Walker, K., Pauly, A., & Randrianambinintsoa, F. J. (2008). Phylogeny of Halictidae with an emphasis on endemic African Halictinae. *Apidologie*, *39*(1), 86-101.

Danforth, B. N., Sipes, S., Fang, J., & Brady, S. G. (2006). The history of early bee diversification based on five genes plus morphology. *Proceedings of the National Academy of Sciences*, *103*(41), 15118-15123.

De Meulemeester, T., Michez, D., Aytekin, A. M., & Danforth, B. N. (2012). Taxonomic affinity of halictid bee fossils (Hymenoptera: Anthophila) based on geometric morphometrics analyses of wing shape. *Journal of Systematic Palaeontology*, *10*(4), 755-764.

de Oliveira, F. F., Mahlmann, T., & Engel, M. S. (2011). A new species of *Chilicola* from Bahia, Brazil (Hymenoptera, Colletidae), with a key to the species of the megalostigma group. *ZooKeys*, *153*, 81-90.

Debevec, A. H., Cardinal, S., & Danforth, B. N. (2012). Identifying the sister group to the bees: a molecular phylogeny of Aculeata with an emphasis on the superfamily Apoidea. *Zoologica Scripta*, *41*(5), 527-535.

Dehon, M., Michez, D., Nel, A., Engel, M. S., & De Meulemeester, T. (2014). Wing shape of four new bee fossils (Hymenoptera: Anthophila) provides insights to bee evolution. *PloS one*, *9*(10), e108865.

Donoghue, M. J., Doyle, J. A., Gauthier, J., Kluge, A. G., & Rowe, T. (1989). The importance of fossils in phylogeny reconstruction. *Annual Review of Ecology and Systematics*, *20*(1), 431-460.

Doyle, J. A., & Donoghue, M. J. (1987). The importance of fossils in elucidating seed plant phylogeny and macroevolution. *Review of Palaeobotany and Palynology*, *50*(1-2), 63-95.

Dunn, C. W., Hejnol, A., Matus, D. Q., Pang, K., Browne, W. E., Smith, S. A., ... & Sørensen, M. V. (2008). Broad phylogenomic sampling improves resolution of the animal tree of life. *Nature*, *452*(7188), 745-749.

Eernisse, D. J., & Kluge, A. G. (1993). Taxonomic congruence versus total evidence, and amniote phylogeny inferred from fossils, molecules, and morphology. *Molecular Biology and Evolution*, *10*(6), 1170-1195.

Engel, M. S. (1999). A new xeromelissine bee in Tertiary amber of the Dominican Republic (Hymenoptera: Colletidae). *Insect Systematics & Evolution*, *30*(4), 453-458.

Engel, M. S. (2001). A monograph of the Baltic amber bees and evolution of the Apoidea (Hymenoptera). *Bulletin of the American Museum of natural History*, 259, 1-192.

Engel, M., & Rightmyer, M. (2000). A new augochlorine bee species in Tertiary amber from the Dominican Republic (Hymenoptera: Halictidae). *Apidologie*, *31*(3), 431-436.

Evenstar, L. A., Stuart, F. M., Hartley, A. J., & Tattitch, B. (2015). Slow Cenozoic uplift of the western Andean Cordillera indicated by cosmogenic 3He in alluvial boulders from the Pacific Planation Surface. *Geophysical Research Letters*, *42*(20), 8448-8455.

Ferdous, S. (2013). Geometric Morphometrics and Phylogeny of the Catfish genus Mystus Scopoli (Siluriformes: Bagridae) and North American Cyprinids (Cypriniformes*)* (Doctoral dissertation, Auburn University, Alabama).

Gaunt, M. W., & Miles, M. A. (2002). An insect molecular clock dates the origin of the insects and accords with palaeontological and biogeographic landmarks. *Molecular biology and evolution*, *19*(5), 748-761.

Gauthier, J., Kluge, A. G., & Rowe, T. (1988). Amniote phylogeny and the importance of fossils. *Cladistics*, *4*(2), 105-209.

Goloboff, P. A., & Catalano, S. A. (2016). TNT version 1.5, including a full implementation of phylogenetic morphometrics. *Cladistics*, *32*(3), 221-238.

Goloboff, P. A., Farris, J. S., Källersjö, M., Oxelman, B., & Szumik, C. A. (2003). Improvements to resampling measures of group support. *Cladistics*, *19*(4), 324-332.

Goloboff, P. A., Mattoni, C. I., & Quinteros, A. S. (2006). Continuous characters analyzed as such. *Cladistics*, *22*(6), 589-601.

González, V. H., & Giraldo, C. (2009). New Andean bee species of *Chilicola* Spinola (Hymenoptera: Colletidae, Xeromelissinae) with notes on their biology. *Caldasia*, *31*(1), 145-154.

González-José, R., Escapa, I., Neves, W. A., Cúneo, R., & Pucciarelli, H. M. (2008). Cladistic analysis of continuous modularized traits provides phylogenetic signals in *Homo* evolution. *Nature*, *453*(7196), 775.

Grimaldi, D. (1999). The co-radiations of pollinating insects and angiosperms in the Cretaceous. *Annals of the Missouri Botanical Garden*, 373-406.

Heath, T. A., Huelsenbeck, J. P., & Stadler, T. (2014). The fossilized birth–death process for coherent calibration of divergence-time estimates. *Proceedings of the National Academy of Sciences*, *111*(29), E2957-E2966.

Hedtke, S. M., Patiny, S., & Danforth, B. N. (2013). The bee tree of life: a supermatrix approach to apoid phylogeny and biogeography. *BMC evolutionary biology*, *13*(1), 138.

Hennig, W. (1966). Phylogenetic Systematics: By Willi Hennig. Transl. by D. Dwight Davis and Rainer Zangerl.

Kayaalp, P., Stevens, M. I., & Schwarz, M. P. (2017). 'Back to Africa': increased taxon sampling confirms a problematic Australia-to-Africa bee dispersal event in the Eocene. *Systematic Entomology*. 42(4), 724–733.

Klingenberg, C. P. (2011). MorphoJ: an integrated software package for geometric morphometrics. *Molecular ecology resources*, *11*(2), 353-357.

Lomholdt, O. (1982). On the origin of the bees (Hymenoptera: Apidae, Sphecidae). *Insect Systematics & Evolution*, *13*(2), 185-190.

Maddison, W. P., & Maddison, D. R. (2001). Mesquite: a modular system for evolutionary analysis.

Melo, G. A. (1999). Phylogenetic relationships and classification of the major lineages of Apoidea (Hymenoptera). Univ. Kansas Nat. Hist. Mus. Sci. Pap 14:1–55.

Michener, C. D. (1944). Comparative external morphology, phylogeny, and a classification of the bees (Hymenoptera). American Museum of Natural History, 82,151–326.

Michener, C. D. (1979). Biogeography of the bees. *Annals of the Missouri botanical Garden*, 66, 277-347.

Michener, C. D. (1992). Mexican and Central American species of Chilicola (Hymenoptera: Colletidae). *Folia Entomológica Mexicana*, *85*, 77-93.

Michener, C. D. (1995). A classification of the bees of the subfamily Xeromelissinae (Hymenoptera: Colletidae). *Journal of the Kansas Entomological Society*, 68(3), 332-345.

Michener, C. D. (2002). The bee genus *Chilicola* in the tropical Andes, with observations on nesting biology and a phylogenetic analysis of the subgenera (Hymenoptera: Colletidae, Xeromelissinae). Natural History Museum, The University of Kansas, 26, 1-47.

Michener, C. D. (2007). The Bees of the World. 2nd. *Ed. Johns Hopkins, Baltimore*.

Michener, C. D., & Grimaldi, D. A. (1988). The oldest fossil bee: Apoid history, evolutionary stasis, and antiquity of social behavior. *Proceedings of the National Academy of Sciences*, *85*(17), 6424-6426.

Michener, C. D., & Poinar Jr, G. (1996). The known bee fauna of the Dominican amber. *Journal of the Kansas Entomological Society*, 69(4), 353-361.

Michez, D, T. De Meulemeester, P, Rasmont, A.Nel, and S, Patiny. (2009) New fossil evidence of the early diversification of bees: Paleohabropoda oudardi from the French Paleocene (Hymenoptera, Apidae, Anthophorini). *Zoologica Scripta* 38(2), 171-181.

Michez, D., Vanderplanck, M., Engel, M. S., & Patiny, S. (2012). Fossil bees and their plant associates. *Evolution of plant-pollinator relationships*, 103-164.

Monckton, S. K. (2016). A revision of *Chilicola* (*Heteroediscelis*), a subgenus of xeromelissine bees (Hymenoptera, Colletidae) endemic to Chile: taxonomy, phylogeny, and biogeography, with descriptions of eight new species. *ZooKeys*, (591), 1-44.

Ohl, M., & Bleidorn, C. (2006). The phylogenetic position of the enigmatic wasp family Heterogynaidae based on molecular data, with description of a new, nocturnal species (Hymenoptera: Apoidea). *Systematic Entomology*, *31*(2), 321-337.

Ohl, M., & Engel, M. S. (2007). *Die Fossilgeschichte der Bienen und ihrer nächsten Verwandten (Hymenoptera: Apoidea)*.

Packer, L. (2008). Phylogeny and classification of the Xeromelissinae (Hymenoptera: Apoidea, Colletidae) with special emphasis on the genus *Chilicola*. *Systematic Entomology*, *33*(1), 72-96.

Perrard, A., Lopez-Osorio, F., & Carpenter, J. M. (2016). Phylogeny, landmark analysis and the use of wing venation to study the evolution of social wasps (Hymenoptera: Vespidae: Vespinae). *Cladistics*, *32*(4), 406-425.

Poinar, G. O., & Danforth, B. N. (2006). A fossil bee from Early Cretaceous Burmese amber. *Science*, *314*(5799), 614-614.

Praz, C. J., & Packer, L. (2014). Phylogenetic position of the bee genera *Ancyla* and *Tarsalia* (Hymenoptera: Apidae): A remarkable base compositional bias and an early Paleogene geodispersal from North America to the Old World. *Molecular phylogenetics and evolution*, *81*, 258-270.

Pyron, R. A. (2011). Divergence time estimation using fossils as terminal taxa and the origins of Lissamphibia. *Systematic Biology*, *60*(4), 466-481.

Ricklefs, R., & Bermingham, E. (2008). The West Indies as a laboratory of biogeography and evolution. *Philosophical Transactions of the Royal Society of London B: Biological Sciences*, *363*(1502), 2393-2413.

Roggero, A., Dierkens, M., Barbero, E., & Palestrini, C. (2016). Combined phylogenetic analysis of two new Afrotropical genera of Onthophagini (Coleoptera, Scarabaeidae). *Zoological Journal of the Linnean Society*, *180*(2), 298-320.

Rohlf, F. J. (1998). On applications of geometric morphometrics to studies of ontogeny and phylogeny. *Systematic Biology*, *47*(1), 147-158.

Rohlf, F. J. (2009). tpsUtil version 1.44. *New York State University at Stony Brook*.

Rohlf, F. J. (2013). tpsDig, v. 2.17. *NY State University at Stony Brook*.

Rohlf, F. J., & Marcus, L. F. (1993). A revolution morphometrics. *Trends in Ecology & Evolution*, 8(4), 129-132.

Rohlf, F. J., & Slice, D. (1990). Extensions of the Procrustes method for the optimal superimposition of landmarks. *Systematic Biology*, *39*(1), 40-59.

Roig-Alsina, A., Michener, C. D., & Silveira, F. A. (1993). Studies of the phylogeny and classification of long-tongued bees (Hymenoptera: Apoidea). *The Univ. of Kansas science bulletin*, 55,123–162.

Ronquist, F., Klopfstein, S., Vilhelmsen, L., Schulmeister, S., Murray, D. L., & Rasnitsyn, A. P. (2012). A total-evidence approach to dating with fossils, applied to the early radiation of the Hymenoptera. *Systematic Biology*, 61(6), 973-999.

Shcherbakov, D. E., Lukashevich, E. D., & Blagoderov, V. A. (1995). Triassic Diptera and initial radiation of the order. *International Journal of Dipterological Research*, *6*(2), 75-115.

Sheets, H. D. (2002). CoordGen 6d. *Freely available at: http://www2/canisius. edu/sheets/morphsoft. html*.

Sheets, H. D. (2003a). CoordGen for integrated morphometrics package, Version 6f. *Department of Physics, Canisius College, Buffalo, NY*.

Sheets, H. D. (2003b). IMP: CVAGen. *Version 6j [computer program]*. *Department of Physics, Canisius College, Buffalo, NY Available from http://www3. canisius. edu/~ sheets/morphsoft. html [accessed 7 November 2008]*.

Webster, M., & Sheets, H. D. (2010). A practical introduction to landmark-based geometric morphometrics. *Quantitative methods in paleobiology*, *16*, 168-188.

Zhang, C., Stadler, T., Klopfstein, S., Heath, T. A., & Ronquist, F. (2015). Total-evidence dating under the fossilized birth-death process. *Systematic biology*, *65*(2), 228-249.